NACA

RESEARCH MEMORANDUM

THEORETICAL AND ANALOG STUDIES OF THE EFFECTS OF NONLINEAR STABILITY DERIVATIVES ON THE LONGITUDINAL MOTIONS OF AN AIRCRAFT IN RESPONSE TO STEP CONTROL DEFLECTIONS AND TO THE INFLUENCE OF PROPORTIONAL AUTOMATIC CONTROL

By Howard J. Curfman, Jr.

Langley Aeronautical Laboratory
Langley Field, Va.

NATIONAL ADVISORY COMMITTEE
FOR AERONAUTICS

WASHINGTON
February 23, 1951

NATIONAL ADVISORY COMMITTEE FOR AERONAUTICS

RESEARCH MEMORANDUM

THEORETICAL AND ANALOG STUDIES OF THE EFFECTS OF NONLINEAR STABILITY DERIVATIVES ON THE LONGITUDINAL MOTIONS OF AN AIRCRAFT IN RESPONSE TO STEP CONTROL DEFLECTIONS AND TO THE INFLUENCE OF PROPORTIONAL AUTOMATIC CONTROL

By Howard J. Curfman, Jr.

SUMMARY

A study has been made of the effects of two nonlinear stability derivatives, caused by the nonlinear variations of pitching-moment and lift coefficients with angle of attack, on the longitudinal motions of an aircraft. Theoretical methods involving the Laplace transformation and the procedures of nonlinear mechanics have been presented along with electrical-analog results for the responses of a canard aircraft to step control deflections and to the influence of two types of proportional automatic control.

In all cases except the example illustrating the procedures of nonlinear mechanics, the nonlinear variations have been approximated by three linear segments. The principal means of studying the effects of the nonlinearities were through the characteristics of the time responses in angle of attack and, in some cases, pitching velocity. The changes in the period and damping of the oscillations due to the nonlinearities have been discussed. The effects of the autopilot proportionality constant on system stability were also investigated. The occurrence of continuous hunting oscillations was predicted and demonstrated for the attitude stabilization system with proportional control for certain nonlinear pitching-moment variations and autopilot adjustments.

INTRODUCTION

In the classical treatments of the study of aircraft dynamics an assumption is usually made that the forces and moments resulting from

small disturbances in position, velocity, and acceleration are linear variations with these quantities. However, some aircraft configurations do not exhibit linear force and moment characteristics in some flight conditions and, therefore, the linearized methods cannot be a satisfactory approximation over an appreciable range of the parameter involved. This paper is concerned with the problem of aircraft dynamics as affected by nonlinear stability derivatives and, in particular, with the short-period longitudinal mode of motion of an aircraft flying at constant velocity. Consideration is also given to the problem of applying simple forms of automatic control to such an aircraft.

The present work is presented in two independent parts. The first part considers several analytical approaches that may be used in the analysis and the study of the transient motions of the aircraft. These methods include the use of the operational calculus (Laplace transformation), the stability criterion of Routh, and the theories of nonlinear mechanics. The second part presents some of the results obtained by using electrical analog equipment. The cases presented are for a hypothetical canard aircraft assumed to be flying at supersonic speed.

SYMBOLS

α angle of attack, positive when nose is above relative wind vector, radians unless otherwise noted

$\dot{\alpha} = \frac{d\alpha}{dt}$

θ aircraft attitude or pitch angle, positive when nose is above horizontal, radians

$\dot{\theta} = \frac{d\theta}{dt}$

δ aircraft elevator deflection angle, positive when trailing edge is down, radians unless otherwise noted

V aircraft velocity, feet per second

q dynamic pressure, pounds per square foot

S wing (reference) area, square feet

$\bar{c}$ mean aerodynamic chord, feet

m mass of aircraft, slugs

I_Y pitching moment of inertia, slug-feet square

D differential operator (d/dt)

t time

C_m pitching-moment coefficient (Pitching moment/$qS\bar{c}$)

C_L lift coefficient (Lift/qS)

$$C_{m_q} = \frac{\partial C_m}{\partial \frac{q\bar{c}}{2V}}$$

$$C_{m_{\dot{\alpha}}} = \frac{\partial C_m}{\partial \frac{\dot{\alpha}\bar{c}}{2V}}$$

$$C_{m_\delta} = \frac{\partial C_m}{\partial \delta}$$

$$C_{L_\delta} = \frac{\partial C_L}{\partial \delta}$$

k_1 slope of a linear segment representing a portion of nonlinear $C_m(\alpha)$ function, per radian

k_2 slope of a linear segment representing a portion of nonlinear $C_L(\alpha)$ function, per radian

a,b,c,d constants used in equations (6) and (9) and defined in appendix

σ,η constants used in equations (2) and (3), respectively

ω_n undamped natural frequency of aircraft alone, radians per second

ζ nondimensional damping ratio of aircraft mode of motion

s Laplace transform variable

K general autopilot constant, ratio of control surface deflection to applied error angle

$$K_1 = \frac{\delta}{\alpha_i - \alpha}$$

$K_2 = \dfrac{\delta}{\theta_i - \theta}$

α_i reference or desired angle of attack for closed-loop system with angle-of-attack feedback, radians

θ_i reference or desired attitude angle for closed-loop attitude-stabilization system, radians

c_0, c_1 constants required in cubic representation of nonlinear $C_m(\alpha)$ function (equation (12))

λ slope of trajectory in phase plane example $(d\dot{\theta}/d\alpha)$

ANALYSIS

The analysis of the effects of nonlinear stability derivatives on the longitudinal motions of a canard aircraft is presented in three sections: the first is a statement of the problem and the assumptions involved; the second is a theoretical or analytical solution for the required transients and the study of stability; and the third is a discussion of the methods of nonlinear mechanics for these dynamical studies.

Statement of Problem

The purpose of this paper is to present methods for determining the nature of the transient responses of aircraft having nonlinear stability derivatives and to show some qualitative results of preliminary investigations.

In the present paper, consideration is given to the longitudinal motions of a canard configuration with the angle-of-attack transients resulting from step elevator deflections serving to illustrate the effects of the nonlinear stability derivatives. Two longitudinal-stability derivatives were considered to have nonlinear characteristics which were caused by the variations of pitching-moment coefficient and lift coefficient with angle of attack. The main emphasis herein was placed on the effects of the nonlinear variation of pitching-moment coefficient with angle of attack since the slope of this curve is a measure of the static stability of the aircraft. Figure 1 illustrates the nature of the nonlinearities under discussion. Such nonlinearities would be apparent from wind-tunnel tests.

In the analysis and study of the aircraft longitudinal motions, two degrees of freedom with constant forward velocity and disturbances from level flight have been assumed. This assumption results in a consideration of the short-period mode of motion only; therefore, only the effects of the nonlinearities on this mode will be apparent.

In addition to studying transients of the aircraft in response to step elevator inputs, consideration was also given to the response characteristics resulting when such an aircraft is subjected to simple forms of automatic stabilization. Two cases were investigated in this respect and are illustrated by block diagrams in figure 2. In both cases the automatic control consists of an error-sensing device and a zero-lag proportional servomotor. In figure 2(a) angle-of-attack stabilization is considered with the control-surface deflection δ being proportional to the difference between a reference angle of attack α_i and the actual angle of attack α. In figure 2(b) attitude stabilization is considered where the control-surface deflection δ is proportional to the difference between a reference attitude angle θ_i and the actual attitude θ.

Theoretical Methods

Equations of motion.- The longitudinal equations of motion of an aircraft having two degrees of freedom with constant forward velocity and disturbances from level flight in terms of the differential operator $D = \frac{d}{dt}$ are

$$\left.\begin{aligned} \frac{I_Y}{qS\bar{c}} D^2\theta - C_{m_q} \frac{\bar{c}}{2V} D\theta - C_m(\alpha) - C_{m_{\dot{\alpha}}} \frac{\bar{c}}{2V} D\alpha &= C_{m_\delta}\delta \\ \frac{mV}{qS} D\theta - \frac{mV}{qS} D\alpha - C_L(\alpha) &= C_{L_\delta}\delta \end{aligned}\right\} \quad (1)$$

The terms which are nonlinear functions of angle of attack are written as $C_m(\alpha)$ and $C_L(\alpha)$ and represent, respectively, the pitching-moment coefficient and lift coefficient that exist at the instantaneous angle of attack.

Based on the usual assumptions of linear variations of C_m and C_L with α, equations (1) remain as ordinary linear differential equations with constant coefficients and are handled by familiar mathematical methods. The types of nonlinearities illustrated in figure 1, however, obviously make linearization of these parameters over the entire range of angle of attack a poor approximation. Since the methods for the

solution of linear differential equations are so well known, an approximation of the nonlinear functions with linear segments, the equations of which can be written for a specified range of angle of attack, seems advisable. Figure 3 is an illustration of this method of representing a nonlinear function. The three straight lines shown are used to represent a variation of pitching-moment coefficient with angle of attack similar to the one shown in figure 1, where the slope at outer α is twice the slope at central α. Each segment of this representation can be expressed as follows:

$$C_m(\alpha) = k_1\alpha + \sigma$$

where k_1 and σ must be specified for each range of angle of attack. In general, therefore, the representation of the nonlinearities are written as

$$C_m(\alpha) = k_1\alpha + \sigma \tag{2}$$

$$C_L(\alpha) = k_2\alpha + \eta \tag{3}$$

where the values of k_1, k_2, σ, and η are constants and apply only for a specified range of angle of attack.

The substitution of equations (2) and (3) into equations (1) results in linear differential equations with constant coefficients, namely,

$$\left.\begin{aligned} \frac{I_Y}{qS\bar{c}} D^2\theta - C_{m_q} \frac{\bar{c}}{2V} D\theta - k_1\alpha - C_{m_{\dot{\alpha}}} \frac{\bar{c}}{2V} D\alpha = C_{m_\delta}\delta + \sigma \\ \frac{mV}{qS} D\theta - \frac{mV}{qS} D\alpha - k_2\alpha = C_{L_\delta}\delta + \eta \end{aligned}\right\} \tag{4}$$

These equations apply only to the region of angle of attack in which the given constants are as defined.

Aircraft transients.- Since variations in angle of attack following step elevator deflections may be in regions where the definition of the nonlinear functions has changed, complete knowledge of the motion is required and solutions of the equations must be written in terms of necessary conditions existing at an arbitrary time. In other words, the values of the angles and their rates of change must be known at the time one set of equations ceases to apply so that the same conditions and, therefore, continuity may be satisfied when the next set of

equations becomes applicable. With these considerations the use of operational methods based on the Laplace transformation affords a means of handling the difficulties already noted and provides the required analytical expressions for the desired transient responses. References 1 to 4 give adequate discussions of the use of the Laplace transformation in the solution of differential equations. Since the usual forms of the Laplace transformation require the initial conditions at zero time, it is convenient to make solutions for the required motions for each range of angle of attack and it may be necessary to redefine the time as zero whenever the equations must be changed because of the representation of the nonlinearities. Such a procedure is obviously time consuming and tedious since solutions for all the parameters are required for a complete definition of initial conditions. A rather complete discussion of this procedure can be found in reference 5.

Closed-loop stability.- The stability of a complete closed-loop system consisting of the aircraft and automatic-control unit, such as illustrated in figure 2, has been theorized by many authors when the system is linear throughout; see, for example, references 2, 6, 7, and 8. Briefly, this procedure is to plot the frequency response (reference 9) of the aircraft as a Nyquist diagram (references 2, 7, and 8) or as an amplitude-phase plot (references 2 and 6) and then to determine the autopilot constant K required to make the system stable and give, as closely as possible, the desired response. Since the frequency-response method requires a completely linear system, such a method cannot be applied in the conventional manner and have meaning because of the definition of the nonlinear functions.

This stability, however, can be examined by the methods of Routh and Hurwitz described in references 10, 11, and 12. This procedure requires the characteristic equations that exist for each region used in the representation of the nonlinear functions. If these investigations indicate stability in all regions of the parametric representation, the stability of the closed loop is generally assured. Such methods could also be used, of course, to determine the values of the autopilot constant K required to assure complete stability.

The application of this technique for the cases of angle-of-attack feedback and attitude stabilization is as follows:

(a) Angle-of-attack feedback: The control equation is written as follows for the angle-of-attack feedback system (see fig. 2(a)):

$$\delta = K_1(\alpha_i - \alpha) \tag{5}$$

When equation (5) is substituted into equations (4) and the Laplace transformations of the resulting expressions are formed, the solution for α can be written in terms of the transform variable as

$$\alpha(s) = \frac{K_1(as^2 + bs)\alpha_i(s) + \left[\text{I.C.}(s)\right]_\alpha}{s\left[s^2 + (2\zeta\omega_n + K_1 a)s + \omega_n^2 + K_1 b\right]} \tag{6}$$

where the term $\left[\text{I.C.}(s)\right]_\alpha$ is the function of s, involving the initial conditions and constants, that results when the control equation and equations (4) have been transformed and solved for $\alpha(s)$, and the other coefficients are constants. These expressions are tabulated in terms of the aircraft parameters in the appendix.

The stability criteria of the characteristic equation of (6) are

$$\left.\begin{aligned} 2\zeta\omega_n + K_1 a > 0 \\ \text{and} \\ \omega_n^2 + K_1 b > 0 \end{aligned}\right\} \tag{7}$$

The inequalities (7) allow a thorough investigation of the effects of K_1 on stability. These criteria must be checked of course in each range of α used in defining the nonlinear functions which appear in equations (1) if the type of motion is to be completely investigated. The types of motion possible are similar to those of a simple spring, mass, viscous damping system which also has a quadratic characteristic equation (see, for example, references 2 and 13). The equation which describes the attitude variations as this type of system operates can be determined by solving for $\theta(s)$ after equations (4) and (5) are transformed as described previously.

The angle-of-attack feedback system does not exhibit a zero error at steady state even for the completely linear case. This condition may be seen by applying the final-value theorem (see, for example, reference 2, pp. 72-73) to equation (6) and noting that the steady-state angle of attack does not equal the input α_i and, hence, the error $\alpha_i - \alpha$ does not tend to zero. This characteristic also is present when the nonlinear functions are considered. For the nonlinearities considered herein, all α transients are completely stable, that is, exhibit steady-state values.

(b) Attitude stabilization: The control equation is written as follows when attitude stabilization is considered (see fig. 2(b)):

$$\delta = K_2(\theta_i - \theta) \tag{8}$$

When equation (8) is substituted into equations (4) and the transformations are made, the complete closed-loop solution for $\theta(s)$ becomes

$$\theta(s) = \frac{K_2(cs + d)\theta_i(s) + \left[\text{I.C.}(s)\right]_\theta}{s^3 + 2\zeta\omega_n s^2 + (\omega_n^2 + K_2 c)s + K_2 d} \tag{9}$$

where $\left[\text{I.C.}(s)\right]_\theta$ is the function of s, involving initial conditions and constants, that results when the control equation and equations (4) have been transformed and solved for $\theta(s)$, and the other factors are constants as defined in the appendix.

The criteria for stability of the cubic characteristic equation of equation (9) require that all coefficients be positive and that

$$(2\zeta\omega_n)(\omega_n^2 + K_2 c) - K_2 d > 0 \tag{10}$$

These criteria allow a complete investigation of the effect of K_2 on stability and should be checked for each angle-of-attack range where definition of the nonlinear functions changes. The angle-of-attack variation $\alpha(s)$ for this system can be solved for from the transformed equations (4) after the control equation (8) is considered.

For the completely linear case when stability is assured, equation (9) reveals that the system is a zero-error system, the output tending to equal the input and the error $(\theta_i - \theta)$ tending to equal zero. For the nonlinearities considered herein, two conditions affecting operation of the system can exist, and these conditions result primarily from the nonlinear $C_m(\alpha)$ function. (For normal $C_L(\alpha)$ functions where the slope remains positive and is not greatly changed in the angle-of-attack regions, this nonlinearity will not affect the stability or oscillatory characteristics to any appreciable extent.) For the system having a nonlinear $C_m(\alpha)$ function and a K_2 satisfying the stability criteria for all values of α, it may be shown from the examination of steady-state α and steady-state θ following a step input θ_i that the system remains a zero-error system. Consider secondly the case where the $C_m(\alpha)$ function has an unstable slope at central α and a stable slope at outer α and a K_2 such that stability is assured at outer α but not at central α. The instability at central α means that the angle-of-attack motion in this region is divergent to outer α; that is, no steady-state α can exist at central α. Upon examination of $\alpha(s)$ it will also be noted that no steady-state α can exist at

outer α; however, the motion at outer α is stable, and the α tends to the region of central α where the motion has been shown to be divergent. This process is summarized as follows:

(1) At central α, the angle-of-attack motion is always divergent to outer α

(2) No steady-state α exists at outer α

(3) The tendency of the motion at outer α is toward the region of central α

It is concluded, therefore, that the angle-of-attack motion should, after some initial transients, become some form of continuous hunting oscillation (nonsinusoidal) rendering the complete system continuously oscillatory. A constant-amplitude constant-period motion would also be suggested from the summary of the angle-of-attack tendencies when examined on an energy basis, an energy balance becoming established between that energy fed in by the unstable mode and that dissipated in the stable regions.

In summary, the attitude-stabilization analysis reveals the following significant facts:

(1) The autopilot proportionality constant K_2 can be adjusted for complete stability at all values of α and renders the system a zero-position-error system for the nonlinearities considered herein.

(2) If the $C_m(\alpha)$ nonlinearity is such that the constant K_2 assures stability at outer α but not at central α, continuous hunting oscillations can exist.

Closed-loop transients.- Equations (6) and (9) are completely expressed when $\alpha_i(s)$ and $\theta_i(s)$ are known. For a step function of unit magnitude,

$$\theta_i(s) = \alpha_i(s) = \frac{1}{s}$$

Upon substitution into the proper equations, the transform function is known and the inverse transformation to $\alpha(t)$ and/or $\theta(t)$ can be determined.

Methods of Nonlinear Mechanics

For the types of nonlinear functions represented in figure 1, the use of a cubic equation is suggested as a possible representation of the

nonlinearity over an adequate range of angle of attack. Such a cubic representation would, of course, make the differential equations of motion of the aircraft nonlinear. To many such problems, however, the methods of nonlinear mechanics have proved a powerful means of satisfactory analysis, although the results are seldom available as the familiar time responses. References 14 and 15 afford very complete discussions of the methods and techniques used in applications of the theory of nonlinear mechanics.

For the present paper a single application of the methods of nonlinear mechanics will be discussed in detail to illustrate the application and usefulness of such methods to the problem considered. For the case chosen and, in general, for the cases where the principles of nonlinear mechanics are readily applicable, the procedure is to rewrite the differential equations of motion into an independent system, that is, into a system of equations in which time appears only as a differential dt. Such a representation is possible for many cases or can be derived by a suitable change in variable. After such a revision, a phase plane can be defined and the characteristics of the motion can be determined by trajectories in this phase plane. The coordinates of the phase plane will usually allow the trajectories to describe successive states that the system may take as time proceeds but will usually not indicate the times at which the various states exist. For example, trajectories of displacement against rate of displacement would be sufficient to describe the successive states of motion of an oscillating system having one degree of freedom. The graphical representation of trajectories in the phase plane is facilitated by the construction of a family of isoclines where each isocline is a locus of points where the trajectories have a given slope (reference 15, pp. 10 and 248). Investigation of the singularities in the phase plane indicates the type of motions which result from given initial conditions, such as steady hunting oscillations or aperiodic or oscillatory responses that are either divergent or convergent. References 16 and 17 are two examples of applications of the techniques of nonlinear mechanics to cases in which an automatic-control component has rendered a system essentially nonlinear.

The example chosen for this discussion is an aircraft having a nonlinear variation of pitching-moment coefficient with angle of attack under the influence of angle-of-attack stabilization, (fig. 2(a)). The following assumptions are made: (1) the other coefficients are constants as listed in the appendix, (2) the reference angle of attack α_i equals zero, and (3) the nonlinear pitching-moment variation has a positive slope for small positive and negative values of angle of attack. As a consequence of the second assumption, the following equation will apply:

$$\delta = -K_1\alpha \tag{11}$$

For the representation of the nonlinear function $C_m(\alpha)$, consider the C_m curve in figure 1 having a positive slope at small value of α. If the α intercepts are symmetrical about $\alpha = 0$, a cubic representation of this curve would take the form

$$C_m(\alpha) = c_o\alpha^3 - c_1\alpha \tag{12}$$

where c_o and c_1 are constants.

Considering a simplified notation for the equations of motion and substituting equations (11) and (12) result in

$$\left.\begin{aligned} a_1D^2\theta + a_2D\theta - c_o\alpha^3 + c_1\alpha &= a_5(-K_1\alpha) \\ b_1D\theta + b_2D\alpha + b_3\alpha &= 0 \end{aligned}\right\} \tag{13}$$

where C_{L_δ} and $C_{m_{\dot\alpha}}$ have been assumed to be zero. The complete definition of constants is given in the appendix. The equations are rewritten as follows to illustrate that they can be reduced to an independent system:

$$\frac{d\dot\theta}{dt} = \frac{-a_2}{a_1}\dot\theta + \frac{c_o}{a_1}\alpha^3 + \left(-\frac{c_1}{a_1} - \frac{a_5K_1}{a_1}\right)\alpha \tag{14a}$$

$$\frac{d\alpha}{dt} = \dot\theta + \frac{-b_3}{b_2}\alpha \tag{14b}$$

where $\dot\theta = \frac{d\theta}{dt}$ and use is made of the equation $b_2 = -b_1$. These equations suggest that the complete motions can be examined by the instantaneous states of α and $\dot\theta$. This idea is also apparent from the Laplace transform procedure suggested in a previous section since initial values of α and $\dot\theta$ are all that are required for a definition of the motion. Therefore, the $\alpha,\dot\theta$ plane is the phase plane for these considerations.

Before actual trajectories are drawn in this plane, a family of isoclines is determined. The slope of any path in the phase plane is $d\dot\theta/d\alpha$ and is determined by the division of equation (14a) by equation (14b). The resulting equation is

$$\frac{d\dot{\theta}}{d\alpha} = \frac{\frac{-\alpha_2}{a_1}\dot{\theta} + \frac{c_o}{a_1}\alpha^3 + \left(-\frac{c_1}{a_1} - \frac{a_5 K_1}{a_1}\right)\alpha}{\dot{\theta} + \frac{-b_3}{b_2}\alpha} \tag{15}$$

If $d\dot{\theta}/d\alpha$ is assigned a constant value λ, equation (15) can be reduced to the form

$$\dot{\theta} = \frac{\frac{c_o}{a_1}\alpha^3 + \left(\frac{b_3}{b_2}\lambda - \frac{c_1}{a_1} - \frac{a_5 K_1}{a_1}\right)\alpha}{\lambda + \frac{a_2}{a_1}} \tag{16}$$

which is the isocline representing the locus of all points in the phase plane where trajectories must have the slope λ.

The singularities of the system are defined as the equilibrium positions (steady-state values) that the system may attain and are determined from equations (14) by using

$$\frac{d\dot{\theta}}{dt} = \frac{d\alpha}{dt} = 0 \tag{17}$$

When the numerical values for the constants as given in the appendix are used, the following equation results for the isoclines:

$$\dot{\theta} = \frac{-309(10)^3\alpha^3 + (4.51\lambda + 257)\alpha}{\lambda + 4.02}$$

where λ is the slope in radians per second per radian. The singularities are found from equations (14) when conditions of equation (17) are imposed and are

(1) $\alpha = 0, \quad \dot{\theta} = 0$

(2) $\alpha = 0.0278$ radian, $\dot{\theta} = 0.1254$ radians per second

(3) $\alpha = -0.0278, \quad \dot{\theta} = -0.1254$

Figure 4 is a plot of the $\alpha, \dot{\theta}$ phase plane and shows some isoclines for various λ. It is important to note that the trajectories or paths which describe the motion have a definite direction that depends on the position in the phase plane. This direction is determined from equations (14) by considering the value of equation (14a) to be a vector

component in the $\dot{\theta}$ direction and the value of equation (14b) to be a vector component in the α direction. The direction of the resultant of these two components is the direction of the trajectory at that point in the phase plane; this resultant vector is termed the phase velocity at that point since the vector components determined from equations (14) are themselves velocities. The arrows shown on the isoclines are not phase velocity vectors but indicate only the direction of the phase velocity on the various isoclines.

Several trajectories are shown in figure 4 for various initial conditions; these were drawn by the graphical method discussed in reference 15 pages 248-252. It is evident from these trajectories and from the directions of phase velocity on the given isoclines that the two singularities ($\pm 1.59^{\circ}$, ± 0.1254) are points of stable equilibrium; that is, the motion following a disturbance will oscillate about and tend to one of these stable states. A singularity of this type is termed (references 15 and 16) a "stable focus" which means that the motion tends to this equilibrium in an oscillatory manner. The other singularity at (0,0) is an unstable equilibrium point. This instability is evidenced by the fact that the slightest disturbance from this point results in a motion to one of the stable foci. This singularity at the origin is termed a "saddle point."

In this brief discussion it is evident that much can be learned about the characteristics of the system without resorting to actual solution of the nonlinear differential equations. The results presented for this case from an inspection of the nature of the phase plane can also be verified by the application of the various theorems presented in references 14 and 15, which allow a determination of the stability of singularities and of such an important property as the existence or nonexistence of steady oscillations in the system. The methods of nonlinear mechanics, however, are relatively new and, in their present state of development, they cannot be expected to handle an extreme variety of problems. The methods become quite involved even for systems having two degrees of freedom in which definition of the motion requires more than two quantities; the methods become almost impossible when more degrees of freedom are introduced.

ANALOG RESULTS AND DISCUSSION

As a part of the investigation of the effects of nonlinear stability derivatives on the transient longitudinal motions of an aircraft, the problem was studied through the use of electrical analog equipment. The analogs employed were the Engine and Control Simulator manufactured by Philbrick Researches, Inc., and the Reeves Electronic Analog Computer

(hereinafter designated the Philbrick Analog and the REAC, respectively), the units being, respectively, at the Lewis Flight Propulsion Laboratory and the Ames Aeronautical Laboratory of the NACA. Descriptions of the analog units are available from various sources, for example, references 18 and 19.

The nonlinearities considered in these studies included both nonlinear functions represented in equations (4), that is, the nonlinear variations of pitching-moment coefficient and lift coefficient with angle of attack. In all problems presented for both analogs, the nonlinear functions were represented by straight-line segments although the methods of representation used in the two analogs differed. The other basic constants used are tabulated in the appendix, and the nonlinear functions are defined when presented. The presentation and discussion of results are given in two sections: (1) aircraft transient responses and (2) closed-loop transient responses. The first section contains analog solutions of the transients in angle of attack (and, in some cases, rate of pitching) resulting from step deflections of the canard elevator control surfaces. The second section presents some solutions for the closed-loop cases shown in figure 2. In both sections various types of nonlinear functions were chosen as being possibly representative of the nonlinearities likely for the assumed canard configuration.

The results from the Philbrick Analog were obtained by photographing an oscilloscope; the REAC results were made with recording elements. The intent of the Philbrick studies was to survey qualitatively a wide range of nonlinear functions by observing and recording the more unusual transient conditions. For this reason high accuracy in aircraft simulation was not required and the results are discussed in this light. In the REAC problems more exact solutions were required, the accuracy in final α and $\dot{\theta}$ transients being estimated at approximately 2 percent and the accuracy of individual REAC components being considerably better.

Aircraft Transient Responses

The analog results presented herein are aircraft transient responses in angle of attack (and pitching velocity) due to step deflections of the canard elevator surfaces. Although only a few nonlinear situations are discussed in detail, the remarks which summarize the paper are based on a much larger number of cases for which analog solutions were obtained.

Case I. Nonlinear $C_m(\alpha)$: $\frac{dC_m}{d\alpha} = nk_1$, $0 < n < 1$, $-2^\circ < \alpha < 2^\circ$; $\frac{dC_m}{d\alpha} = k_1$, $\alpha < -2^\circ$, $\alpha > 2^\circ$.- In case I the nonlinear function is the

pitching-moment coefficient due to angle of attack where the slope at values of α less than -2° and greater than 2° is larger than the value of the slope in the region $-2^\circ < \alpha < 2^\circ$. In this case, the slope is always negative and stability is assured. Since the frequency of the transient oscillations is determined principally by this slope, changes in the frequency (period) are expected as the region in which the value of the steady-state angle of attack changes because of various elevator deflections. Little change in the damping envelope is expected.

Results from the Philbrick Analog are presented in figure 5. In this run the value of k_1 was equal to -5.14 and the slope for $-2^\circ < \alpha < 2^\circ$ is $0.463k_1 = -2.38$. The α transient shown in figure 5(a) is the completely linear case where $C_m(\alpha) = k_1\alpha$. The total transient time shown represents 1.325 seconds. When the described nonlinearity in $C_m(\alpha)$ is introduced, the results are shown by the four remaining records of figure 5. Curves of figures 5(b) and 5(d) are two α transients, whereas curves of figures 5(c) and 5(e) are the corresponding nonlinearities. These nonlinearities were photographed by using the output of the element generating the nonlinear function as the vertical coordinate of the oscilloscope and the angle of attack as the horizontal coordinate. Hence, the region of angle of attack covered in the transients of figures 5(b) and 5(d) is shown again by the region of the nonlinearity pictured. The large spots shown on the nonlinearities represent the trim values of α due to the old and new δ input. Hence, figure 5(c) shows that the values of δ change in such a way as to make the trim values of α change from one extreme of the nonlinearity to the other. Since the slopes at these outer values of α are the same as that shown for the linear case, the period should remain practically unchanged (compare figs. 5(a) and 5(b)).

Figure 5(d) is the α transient when the change in δ causes the trim α to change from a point where the slope is large to one in the region of reduced slope. The ratio increase in period (reduction in frequency) shown in figure 5(d) is approximately equal to the theoretical variation of being inversely proportional to the square root of the decrease in slope. (This variation will apply for lightly damped systems.) For the three transients shown, the damping envelope is seen to be essentially unchanged, the time required to reach steady state being about 1 second in each case.

Two solutions from the REAC for this case (reproductions of actual recordings) are presented in figure 6. For these solutions the value of k_1 was -6.0 and $n = 0.5$, and the cases shown are the results of moving the elevator in a programmed manner from 0° to about 8° and after steady state is reached to about -4°. The variations of $\dot{\theta}$, α, and δ with time are shown in this figure. The slight phase difference between

control motion and the transients in the REAC solutions are due to the recording equipment and not to aircraft dynamics. The $\pm 2^{\circ}$ (± 0.035 radian) positions noting the break points in the nonlinearity are also indicated on the α transient. The same general characteristics are observed for these two transients as mentioned previously, namely, the change in period and approximately the same time required for both transients to reach steady state. The steady-state values for α and $\dot{\theta}$ check reasonably well with those predicted theoretically. In figure 6 the responses show clearly that when the angle-of-attack variations are such as to be in the region of breaks in the nonlinearity, the periodicity is not constant; when they, however, are in an α region where the slope of the nonlinearity is constant (near steady state), the period does remain constant. For cases such as this illustration where it is relatively certain that the system is very lightly damped, this change in periodicity and finally a constant period near steady state can be attributed to a nonlinearity in the effective spring constant of the system, in this case $C_m(\alpha)$.

Case II, Nonlinear $C_m(\alpha)$: $\frac{dC_m}{d\alpha} = k_1$, $\alpha < -2^{\circ}$, $\alpha > 2^{\circ}$; $\frac{dC_m}{d\alpha} = -nk_1$, $0 < n < 1$, $-2^{\circ} < \alpha < 2^{\circ}$.- In case II the variation of the pitching-moment coefficient with angle of attack is nonlinear and considered to have a positive (unstable) slope in the range $-2^{\circ} < \alpha < 2^{\circ}$. A trim angle of attack for a given elevator deflection (δ) cannot be expected to exist in the region $-2^{\circ} < \alpha < 2^{\circ}$ since in this angle-of-attack region the transients are divergent. (This condition is shown by the presence of two real roots of opposite signs of the quadratic characteristic equation of equations (4), the negative root indicating a damped subsidence and the positive root indicating the divergent aperiodic mode.)

Figure 7 presents some Philbrick solutions for this case where $k_1 = -0.838$, $n \approx 1$. The total transient time shown represents 2.13 seconds. The α transient shown in figure 7(a) is for the completely linear case with $C_m(\alpha) = k_1\alpha$. The period of the damped oscillation is 0.284 second. Figures 7(b), 7(d), and 7(f) are α transients for different δ conditions, and figures 7(c), 7(e), and 7(g) are the parts of the nonlinear function involved in each transient.

From the nonlinearity shown in figure 7(c) the change in trim angle of attack is large with the new trim angle of attack well into the region of stable slope. Therefore, little change is expected or noted in the transient of figure 7(b) as compared with the linear case in figure 7(a). As the value of δ is changed and the new trim angle of attack comes nearer to the break in the nonlinearity (see fig. 7(e)), the initial portion of the transient of figure 7(d) has become distorted.

The characteristics of the oscillations about the new trim angle of attack, however, remain unchanged. As the δ is changed only slightly, a new trim angle of attack is found to the left of the region of unstable slope as shown in figure 7(g). The first overshoot of this transient (fig. 7(f)) is to an angle of attack in the unstable region, but the energy of the system is such that the complete unstable region is not traversed and the oscillatory characteristics about the new trim position become established.

Only a very slight change in the δ was found to be required for the change in trim angle of attack exhibited in the transients of figures 7(d) and 7(f). Only when the new trim angle of attack was near the breaks in the nonlinearities did the transients indicate any peculiarities which might give an indication of the presence of a nonlinearity in the system.

The REAC solutions presented in figure 8 for this case are for a value of $k_1 = -3.0$, $n = 0.5$. The two examples shown start from the same values of δ, trim α, and $\dot{\theta}$ with the first changing from $\delta \approx 4^\circ$ to $\delta \approx -2^\circ$ and the second changing to $\delta \approx -4^\circ$. In both of these conditions, the angle-of-attack variations are from a point of stable equilibrium at positive α to a stable trim position at negative α. The transients indicate that the initial portions give the only hint of nonlinearity in the system. As noted previously, this initial part of the α transients becomes more out of the ordinary as the new position of trim α approaches the break point of the nonlinearity. These slight slope changes in the α transient are almost unnoticeable in the second curve. Examination of the $\dot{\theta}$ transients, however, indicate clearly the effect of the nonlinearity on the rate of pitching in the initial phase of the response. After this first effect on the transients, the oscillatory characteristics become very regular.

Case III. Nonlinear $C_L(\alpha)$: $\frac{dC_L}{d\alpha} = k_2$, $\alpha < -2^\circ$, $\alpha > 2^\circ$; $\frac{dC_L}{d\alpha} = nk_2$, $0 < n < 1$, $-2^\circ < \alpha < 2^\circ$.- In case III the variation of lift coefficient with angle of attack is the nonlinear function having a larger slope at the outer values of α. Since the aircraft is lightly damped, the primary contribution of the lift-curve slope to the oscillatory characteristics is in the damping of the motion. Since, for this case, the slope of the pitching-moment-coefficient curve against angle of attack is a constant $\left(\frac{dC_m}{d\alpha} = k_1\right)$, no change is to be expected in the period of the transient oscillations.

In figure 9 three Philbrick solutions are shown. Figure 9(a) is the completely linear case with $k_2 = 3.49$ $(n = 1)$ and $k_1 = -1.90$.

The transient time is 2.48 seconds, the period is 0.194 second, and the cycles to damp to one-tenth amplitude are 3.39. Figure 9(b) is the transient which results when the trim α changes from a region of large slope ($dC_L/d\alpha$) to a region of α of reduced slope. The value of n is 0.328 in this instance, that is, the slope at central α is about one-third of the slope at outer α. The period is essentially unchanged although the number of cycles to damp to one-tenth amplitude has increased to 4.20. For a change in trim α from the region of reduced slope to the region where the slope is the same as the linear case, the transient in figure 9(c) is practically the same as the one shown in figure 9(a) for the linear case.

The change in slope used in this example is much greater than would be expected in a practical case; thus this change indicates that the actual effects of this parameter might result in very little change in the α transient characteristics. It is also emphasized that a simple examination of the transient (or even a comparison between figs. 9(b) and 9(c)) could not indicate that the nonlinearity was in lift-curve slope because the effect of variation of damping in pitch C_{m_q} would also be manifested by changing the damping but not affecting the period. In actual flight tests, however, normal-acceleration records might help to isolate this effect as a nonlinear $C_L(\alpha)$.

The REAC solutions shown in figure 10 have $k_2 = 4.19$ and $n = 0.834$. The linear equation of $C_m(\alpha) = -3.0\alpha$ was also used in these runs. The variations of δ shown were from $\delta = 0^\circ$ to $\delta \approx 8^\circ$ to $\delta \approx -4^\circ$. The periodicity is constant for these cases even though the variations of α in the second run are about the break point ($\alpha = -0.035$ radian) of the nonlinearity. Since the two slopes of the nonlinear $C_L(\alpha)$ function are nearly the same, the damping is practically unaffected in the two cases; in fact, plots of the logarithm of the peak amplitudes about steady-state values against time for these two cases indicate essentially the same slope and, therefore, the same damping, although the second run has a slight amount of scatter in the points. These cases which have a more reasonable value for n than used in the Philbrick solutions indicate the slight effects of this parameter under the conditions investigated.

Case IV. Nonlinear $C_m(\alpha)$ and $C_L(\alpha)$.- In case IV the two nonlinearities used in the REAC solutions for cases I and III were used together in the same run for two transient solutions. These results are shown in figure 11 for δ changes of 0° to 4° and 0° to 8°. In the first transient only the first overshoot is greater than $\alpha = 2^\circ$, the break point of the nonlinearities; hence, the transient characteristics are those defined entirely by the slopes of the nonlinearities at small α. In the second transient the period becomes constant after the first two cycles and exhibits characteristics similar to that of the first transient of figure 6 with the single nonlinear function $C_m(\alpha)$.

These results might have been expected since the nonlinear $C_L(\alpha)$ had so little effect in case III. Other runs for cases where two nonlinearities were in the system indicated that the most noticeable changes in the transients occurred with changes in the $C_m(\alpha)$ function, as indicated previously.

Review of effects of nonlinearities on aircraft transients.- Nonlinear variations of the pitching moment resulted almost solely in effects on the period of the transient oscillations. Differences in the period of the oscillations in the different regions of angle of attack, due to the different slopes of the nonlinear function in these regions, were an effective way of noting the presence of this nonlinearity. Another noticeable effect was the irregularity in the period of the oscillations when the trim angle of attack for the various elevator deflections was near a break point of the nonlinearity. When the trim angle of attack is removed from the break in the nonlinearity, the oscillation characteristics become very regular, that is, constant period and damping. If only moderate changes in trim angle of attack result from the control motion and the nonlinearity or a part thereof is traversed, the initial sections of the transients may indicate the presence of the nonlinearity through small slope variations, although the final oscillatory characteristics are quite regular. For large changes in trim angles of attack under the conditions noted, the small variations in the initial sections of the transient may become so slight as to be indistinguishable from the perfectly linear case.

For cases when the nonlinear variation was in lift coefficient, large slope changes were required before changes in the oscillatory characteristics became appreciable for trim angles of attack in the different regions. This nonlinearity affected only the damping characteristics of the motions, the period remaining constant. This effect could be expected since very large changes in damping would be required to alter the period of this lightly damped system.

When the two nonlinearities were considered simultaneously, with reasonable variations in each, the predominant changes in transient characteristics were similar to those noted for the single nonlinear pitching-moment variation, that is, the changes in periodicity previously mentioned with the time to damp remaining essentially unaltered.

Closed-Loop Transient Responses

The results in this section are transient response curves illustrating the dynamics of the two closed-loop systems depicted in figure 2. The discussion will be in two parts: the closed loop with angle-of-attack feedback and the attitude stabilization, and includes Philbrick and REAC solutions for several cases. The nonlinear characteristics

will be those previously described for the aircraft; the error-sensing devices and proportional servomotors are considered as zero-lag systems. The transients are the responses to step input, command signals in α_i and θ_i.

Angle-of-attack feedback.- The block diagram for this case is shown in figure 2(a). Transients from the Philbrick Analog are shown for two cases: one where the nonlinear function is $C_L(\alpha)$ and the other for the nonlinearity $C_m(\alpha)$. REAC solutions were made for two different nonlinear functions of pitching-moment coefficient.

In the Philbrick solutions the value of K_1 was approximately unity. For the case with nonlinear $C_L(\alpha)$, the conditions are the same as described for case III of the previous section where the lift-curve slope at outer values of α is greater than the slope at small values of α. The transients shown in figure 12 resulted from changes in α_i that caused the final values of α to be in regions where the lift-curve slope is different. Figure 12(a) shows the α transient about a steady-state value of α in the region where the lift-curve slope is reduced. The oscillations in figure 12(b) are about a steady-state value of α in an α region of larger lift-curve slope. The increase in lift-curve slope is seen to improve the damping characteristics of the closed-loop system with angle-of-attack feedback in much the same way as the aircraft transients were improved. Investigation of the characteristic equation of this closed loop, the denominator of equation (6), shows that the principal effect of such a change in lift-curve slope would be most evident in the damping. Comparison of transients of figure 12 as well as an examination of the characteristic equation indicated that the frequency of the oscillations is constant.

The Philbrick solutions with nonlinear $C_m(\alpha)$ were made for the case where the slope of the pitching-moment-coefficient curve was positive (unstable) at small α and stable at outer α. The outer slopes were -1.90, and the center slope was 0.655. Two α transients illustrating the effects of this nonlinearity on the closed-loop responses are given in figure 13. In figure 13(a) the change in reference angle α_i results in a change in the steady-state values of α from one region of stable slope to the other. In figure 13(b) the input change causes the final value of α to be a value in the region of angle of attack where the aircraft has an unstable pitching-moment curve, and the transient is satisfactory. The physics of this change is explained by the action of the angle-of-attack feedback causing the control surface deflection δ to give a moment proportional to the instantaneous α; thus, this moment adds to the effective spring constant of the system. In this instance, the value of K_1 is large enough so that this contribution overcomes the destabilizing effect of the spring in the aircraft at central α and renders the over-all system stable in this region of α. This stability could also be determined from the

inequalities (7) which show that the value of K_1 used assures complete stability of this closed-loop system.

REAC solutions were also made for a case where the pitching-moment curve had an unstable slope at small values of angle of attack. The same conditions as discussed for REAC runs in case II were used here with a value of $\frac{dC_m}{d\alpha} = -3.0$ for the stable slopes at outer α and $\frac{dC_m}{d\alpha} = 1.5$ for $-2^\circ < \alpha < 2^\circ$. The value of K_1 was 1.0. The three α transients of figure 14 are for the α_i step inputs of 1°, 4°, and 8°. The 2° position noting the break in the nonlinearity is shown on each curve. For this case, an examination of the inequalities (7) reveals that the value of $K_1 = 1.0$ is not large enough to assure complete stability in the region $-2^\circ < \alpha < 2^\circ$; hence, no steady-state value of α is possible in this region. Therefore, for even the small input $\alpha_i = 1^\circ$, the final value of α is greater than the break point of the nonlinearity. The measured values of steady-state α due to the inputs involved are 2.49°, 3.21°, and 4.24° compared to the theoretical values of 2.50°, 3.26°, and 4.30°, respectively. Since the value of α is greater than 2° after the first cycle for all the transients shown, the period of the oscillations is essentially the same for all cases.

The final REAC solutions are shown for the case where the $C_m(\alpha)$ nonlinearity is the same as case I; namely, $\frac{dC_m}{d\alpha} = -3.0$ where $-2^\circ < \alpha < 2^\circ$ and $\frac{dC_m}{d\alpha} = -6.0$ when $\alpha < -2^\circ$, $\alpha > 2^\circ$. The α_i inputs were again 1°, 4°, and 8°, and the value of K_1 was 1.0. The resulting closed-loop α transients are given in figure 15. In these runs too, the steady-state values of α check satisfactorily with the theoretical values. Note that figure 15(c) for $\alpha_i = 8^\circ$ has a final value for α of about 2°; hence, the oscillations are about the break point of the nonlinearity. The period of this transient is very constant and is different from the period of figures 15(a) and 15(b) which both remain in the region $0 < \alpha < 2^\circ$. The period of figures 15(a) and 15(b) is about 1.17 times the period of figure 15(c). A theoretical value of the change in period, obtained from consideration of the values defined by the two slopes of $C_m(\alpha)$, is 1.15; this value is close to the measured value even though the oscillations were not in the region where this result could be expected to apply. Stability of the combination of the aircraft and autopilot with control proportional to angle of attack was obtained by adjustment of the autopilot proportionality constant, and the effects of the nonlinearities were similar to those noted for the aircraft transients to step control deflections.

Examination of figures 14 and 15 indicates that all the cases shown with nonlinearities in the system exhibit a steady-state error between the reference α_i and the actual α. This characteristic is not due primarily to the nonlinearities of the system. An investigation of a linear aircraft in this system of angle-of-attack feedback reveals that the complete system is not a zero-position-error system; therefore, unless some form of compensation is included in the loop the output will not equal the input at steady state. For the cases shown, however, adequate compensation of the system with nonlinearities as described may be no more difficult than that required to make the linear system a zero-position-error-system.

Attitude stabilization:- In the results (REAC) to be presented for the problem of attitude stabilization, the only nonlinearity considered was $C_m(\alpha)$. In the first example the $C_m(\alpha)$ function used for REAC solutions for case I, $dC_m/d\alpha$ being negative for all α but having a larger slope at outer α, was employed. The second example is the $C_m(\alpha)$ function for case II, $dC_m/d\alpha$ having a stable (negative) slope at outer α and an unstable slope at $-2^\circ < \alpha < 2^\circ$ and a K_2 which does not assure stability at central α. The analysis in previous sections indicated that the first example should exhibit constant steady-state values after transients die out, whereas the second example should show continuous hunting oscillations. For both cases $K_2 = 1.0$.

Figure 16 illustrates the first example where the $C_m(\alpha)$ has a negative slope at all α. Figure 16(a) is for $\theta_i = 4.6^\circ$ and figure 16(b) is for $\theta_i = 9^\circ$. The upper curves in figure 16(a) and figure 16(b) are the α variations, whereas the lower curves are of the error $(\theta_i - \theta)$. In both of these cases the error tends to zero indicating the zero position error characteristic of the system. The cubic characteristic equation of this system, see equation (9), would show an oscillatory mode of motion superimposed upon the convergent aperiodic mode and is indicated by the negative real root. From the characteristics of the system at central α, the oscillatory mode damps to one-half amplitude in about one-third of the time required for the aperiodic mode to damp the same amount. In figure 16(b), the period becomes constant only after the variations of α become less than 2°, whereas in figure 16(a) the period is constant throughout.

The results for the second example where the $C_m(\alpha)$ function had an unstable slope in the region $-2^\circ < \alpha < 2^\circ$ are presented in figure 17. Curves in figures 17(a), 17(b), and 17(c) were results of step inputs of θ_i of 0.7°, 4.6°, and 8.7°, respectively. In each set the time variations of α and $(\theta_i - \theta)$ are shown. Though the initial portions of the responses are different for the three cases, the resulting hunting oscillations are essentially the same. These curves show the constant-amplitude constant-period oscillations predicted in the theoretical analysis for this type of nonlinearity.

Stability of the attitude-stabilization system, when the control surface deflection is proportional to the error in attitude, could be completely assured for the types of nonlinearities considered herein with proper adjustment of the autopilot proportionality constant. The existence of continuous hunting oscillations for a particular nonlinear pitching-moment variation and improper autopilot adjustment was predicted theoretically and demonstrated by analog solutions. The pilot of a conventional aircraft might apply control in a manner that is approximately proportional, though probably with a time lag, and such a hunting oscillation as described might be realized if that aircraft had a characteristic like the nonlinearity in the data of figure 17.

CONCLUSIONS

This study has been concerned with the effects of two nonlinear stability derivatives, caused by the nonlinear variations of pitching-moment and lift coefficients with angle of attack, on the longitudinal motions of an aircraft. In addition to the theoretical methods discussed, the excellent adaptation of analog equipment to this dynamical study gave results for the responses of a canard aircraft to step control deflections and to the influence of two types of proportional automatic control. From the theoretical considerations and the analog results presented herein, the following conclusions summarize the investigation:

1. When the nonlinear functions are approximated by a series of linear segments, the methods of the Laplace transformation allow the transient responses of the aircraft alone and also with proportional automatic control to be calculated. The computational procedure required, however, is tedious and time consuming.

2. The most noticeable effects of the nonlinear pitching-moment variations on the response of the aircraft to step control deflections was in the periodicity of the oscillations. The occurrence of an irregular period and of different constant-period oscillations about the various trim angles of attack was the most satisfactory way of noting the presence of this nonlinearity.

3. Nonlinearity in the lift curve affected only the damping of the transient angle-of-attack oscillations, the period remaining constant. Large slope changes in this nonlinear function were required before the effect on the time to damp became appreciable.

4. Simultaneous occurrence of the two types of nonlinearities considered herein, with reasonable values of each, resulted in transient characteristics which were similar to those with the single nonlinear pitching-moment function.

5. Stability of the combination of the aircraft and autopilot with control proportional to angle of attack was obtained by adjustment of the autopilot proportionality constant, and the effects of the nonlinearities were similar to those noted for the aircraft transients to step control deflections.

6. Stability of the attitude-stabilization system, when the control surface deflection is proportional to the error in attitude, could be completely assured for the types of nonlinearities considered herein with proper adjustment of the autopilot proportionality constant. The existence of continuous hunting oscillations for a particular nonlinear pitching-moment variation and improper autopilot adjustment was predicted theoretically and demonstrated by analog solutions.

Langley Aeronautical Laboratory
National Advisory Committee for Aeronautics
Langley Field, Va.

APPENDIX

FACTORS AND COEFFICIENTS USED IN THE ANALYSIS

The complete expressions for the factors and coefficients used in the analysis section of the paper, in the order in which they appear in the text are as follows:

$$a = \frac{b_4}{b_2}$$

$$b = \frac{a_2 b_4}{a_1 b_2} + \frac{a_5}{a_1}$$

$$\left[I.C.(s)\right]_\alpha = \alpha(0)s + \left[\frac{a_2 + a_4}{a_1}\alpha(0) + \dot{\theta}(0) + \frac{\eta}{b_2}\right]s + \frac{\sigma}{a_1} + \frac{a_2\eta}{a_1 b_2}$$

$$2\zeta\omega_n = \frac{a_2}{a_1} + \frac{a_4}{a_1} + \frac{k_2}{b_1}$$

$$\omega_n^2 = -\frac{a_2 k_2}{a_1 b_2} - \frac{k_1}{a_1}$$

(When $\omega_n^2 > 0$ and $2\zeta\omega_n > 0$, ω_n corresponds to the undamped natural frequency of the short-period mode of motion of the aircraft alone and ζ represents the conventional nondimensional damping ratio.)

$$c = \frac{a_5}{a_1} - \frac{a_4 b_4}{a_1 b_2}$$

$$d = -\frac{a_5 k_2}{a_1 b_2} + \frac{k_1 b_4}{a_1 b_2}$$

$$\left[\text{I.C.}(s)\right]_\theta = \theta(0)s^2 + \left[\theta(0)\left(\frac{a_4}{a_1} + \frac{a_2}{a_1} + \frac{k_2}{b_1}\right) + \dot{\theta}(0)\right]s + \theta(0)\left(-\frac{a_2k_2}{a_1b_2} - \frac{k_1}{a_1}\right) +$$

$$\dot{\theta}(0)\left(\frac{k_2}{b_1}\right) + \alpha(0)\left(-\frac{a_4k_2}{a_1b_2} + \frac{k_1}{a_1}\right) + \frac{b_2\sigma - a_4\eta}{a_1b_2} + \frac{1}{s}\left(\frac{-k_2\sigma + k_1\eta}{a_1b_2}\right)$$

$$a_1 = \frac{I_Y}{qS\bar{c}}$$

$$a_2 = -C_{m_q}\frac{\bar{c}}{2V}$$

$$a_4 = -C_{m_{\dot{\alpha}}}\frac{\bar{c}}{2V}$$

$$a_5 = C_{m_\delta}$$

$$b_1 = -b_2 = \frac{mV}{qS}$$

$$b_4 = C_{L_\delta}$$

Values used for example of method of nonlinear mechanics are as follows:

$$c_o = -546$$

$$c_1 = -1.5$$

$$a_1 = 0.00177$$

$$a_2 = 0.00712$$

$$a_4 = 0$$

$$a_5 = 1.045$$

$$b_1 = -b_2 = 0.774$$

$$b_4 = 0$$

$$b_3 = -\frac{dC_L}{d\alpha} = -3.49$$

$$K_1 = 1.0$$

For the solutions made on the Philbrick and Reeves Analog equipment, the numerical values for the aforementioned constants a_1, a_2, a_4, a_5, b_1, b_2, and b_4 were used. The values for these coefficients resulted from the following flight conditions and stability derivatives:

Mach number = 1.8

$V = 2009$ ft/sec

$q = 4800$ lb/ft^2

$S = 2.52$ ft^2

$\bar{c} = 1.4$ ft

$I_Y = 30$ slug-ft^2

$m = 4.66$ slugs

$$C_{m_q} = \frac{\partial C_m}{\partial \frac{qc}{2V}} = -20.43$$

$$C_{m_\delta} = \frac{\partial C_m}{\partial \delta} = 1.045$$

$$C_{L_\delta} = C_{m_{\dot{\alpha}}} = 0$$

REFERENCES

1. Churchill, Ruel V.: Modern Operational Mathematics in Engineering. McGraw-Hill Book Co., Inc., 1944.

2. Brown, Gordon S., and Campbell, Donald P.: Principles of Servomechanisms. John Wiley & Sons, Inc., 1948.

3. Mokrzycki, G. A.: Application of the LaPlace Transformation to the Solution of the Lateral and Longitudinal Stability Equations. NACA TN 2002, 1950.

4. Gardner, Murray F., and Barnes, John L.: Transients in Linear Systems Studied by the Laplace Transformation. Vol. I, John Wiley & Sons, Inc., 1942.

5. Sternfield, Leonard: Some Effects of Nonlinear Variations in the Directional-Stability and Damping-in-Yawing Derivatives on the Lateral Stability of an Airplane. NACA TN 2233, 1950.

6. James, Hubert M., Nichols, Nathaniel B., and Phillips, Ralph S.: Theory of Servomechanisms. McGraw-Hill Book Co., Inc., 1947.

7. Nyquist, H.: Regeneration Theory. Bell Syst. Tech. Jour., vol. XI, no. 1, Jan. 1932.

8. Hall, Albert C.: The Analysis and Synthesis of Linear Servomechanisms. The Technology Press, M.I.T., 1943.

9. Greenberg, Harry: Frequency-Response Method for Determination of Dynamic Stability Characteristics of Airplanes with Automatic Controls. NACA Rep. 882, 1947.

10. Routh, Edward John: Dynamics of a System of Rigid Bodies. Part II. Sixth ed., rev. and enl., Macmillan and Co., Ltd., 1905.

11. Weiss, Herbert K.: Theory of Automatic Control of Airplanes. NACA TN 700, 1939.

12. Sternfield, Leonard: Effect of Automatic Stabilization on the Lateral Oscillatory Stability of a Hypothetical Airplane at Supersonic Speeds. NACA TN 1818, 1949.

13. Den Hartog, J. P.: Mechanical Vibrations. Second ed., McGraw-Hill Book Co., Inc., 1940.

14. Minorsky, N.: Introduction to Non-Linear Mechanics. Edwards Brothers, Inc., 1947.

15. Andronow, A. A., and Chaikin, C. E.: Theory of Oscillations. Princeton Univ. Press, 1949.

16. Weiss, Herbert K.: Analysis of Relay Servomechanisms. Jour. Aero. Sci., vol. 13, no. 7, July 1946, pp. 364-376.

17. Barnes, Frank Arthur: Stability Study of Aircraft Roll-Control Systems Having Power-Limitations and Other Non-Linearities. M.I.T. Thesis, 1949.

18. Philbrick, G. A., Stark, W. T., and Schaffer, W. C.: Electronic Analog Studies for Turboprop Control Systems. SAE Quarterly Trans., vol. 2, no. 2, April 1948.

19. Frost, Seymour: Compact Analog Computer. Electronics, vol. 21, no. 7, July 1948, pp. 116-122.

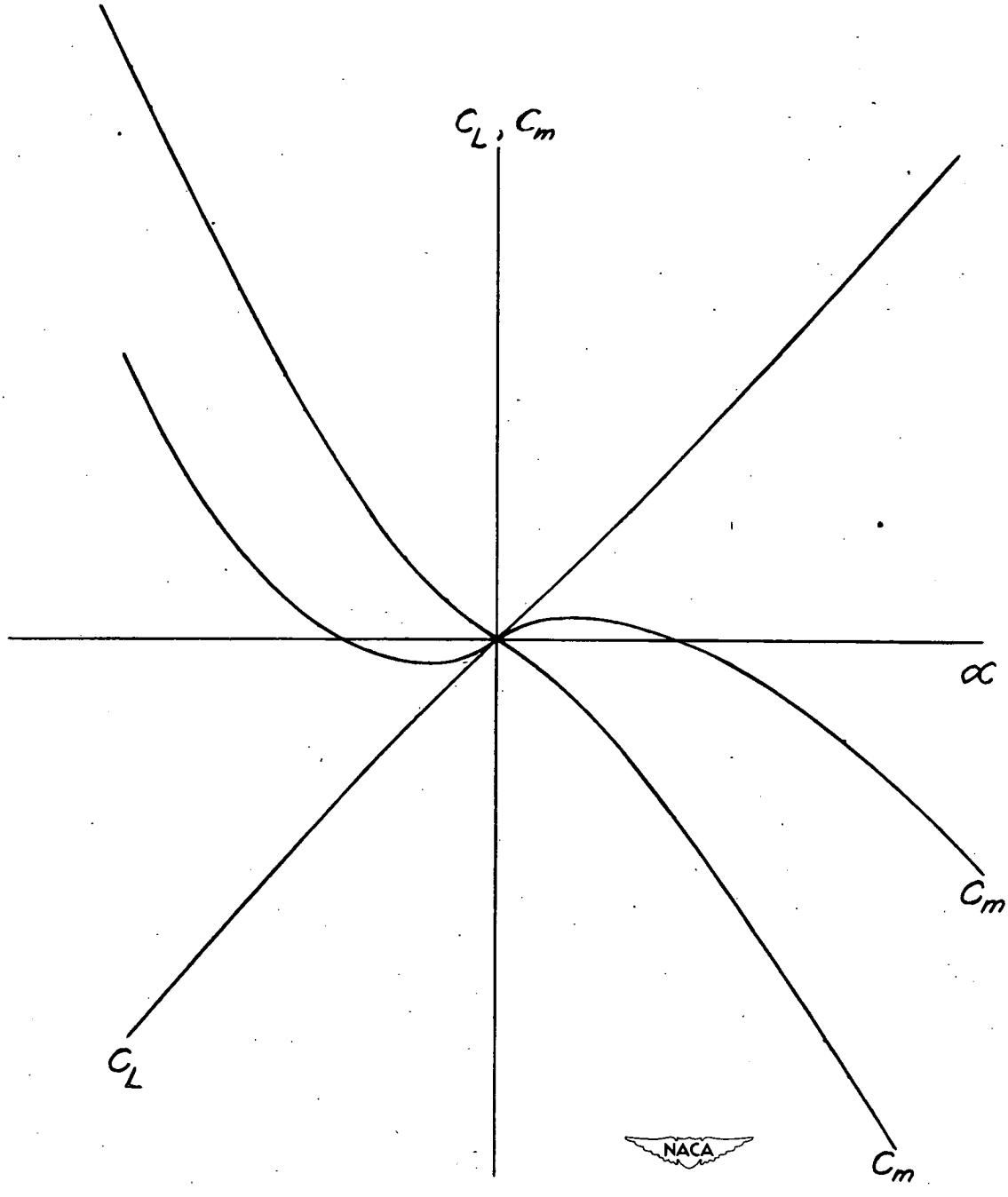

Figure 1.- Typical nonlinearities in pitching-moment and lift coefficients.

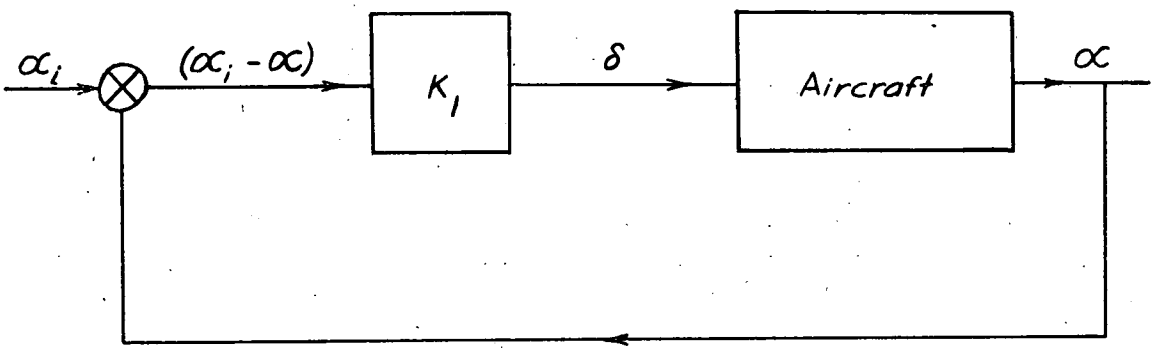

(a) Angle-of-attack stabilization.

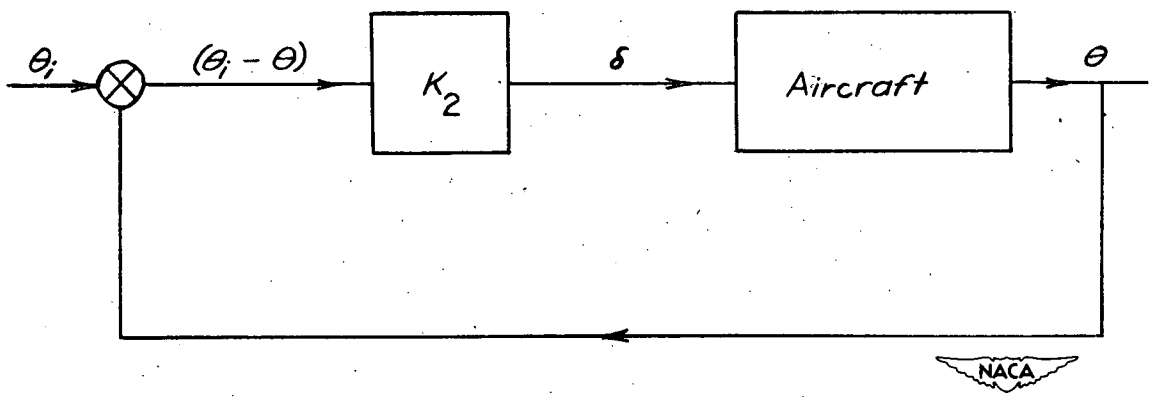

(b) Attitude stabilization.

Figure 2.- Block diagrams illustrating the two types of proportional automatic control under consideration.

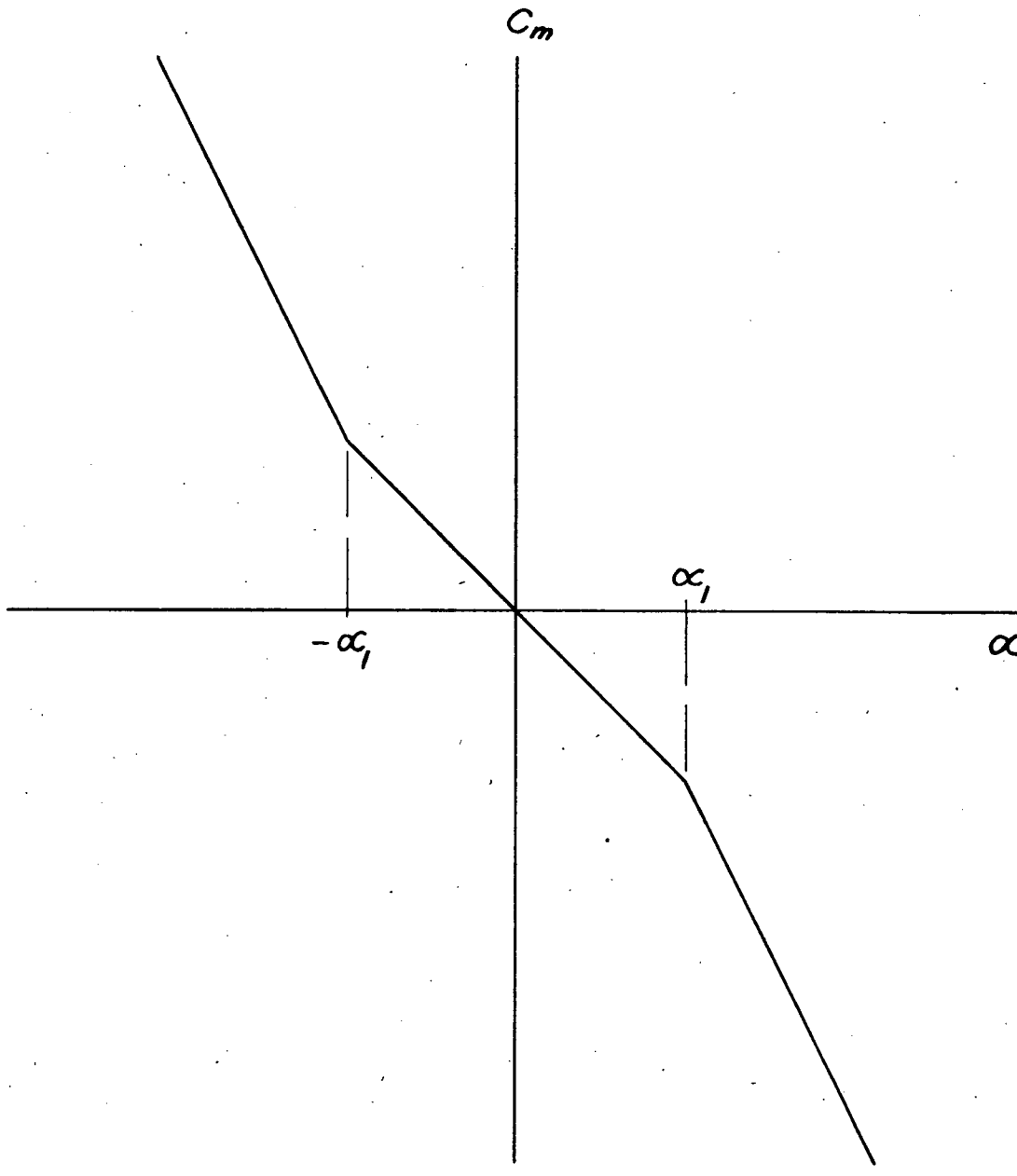

Figure 3.- Illustration of the method of approximating nonlinear functions with linear segments.

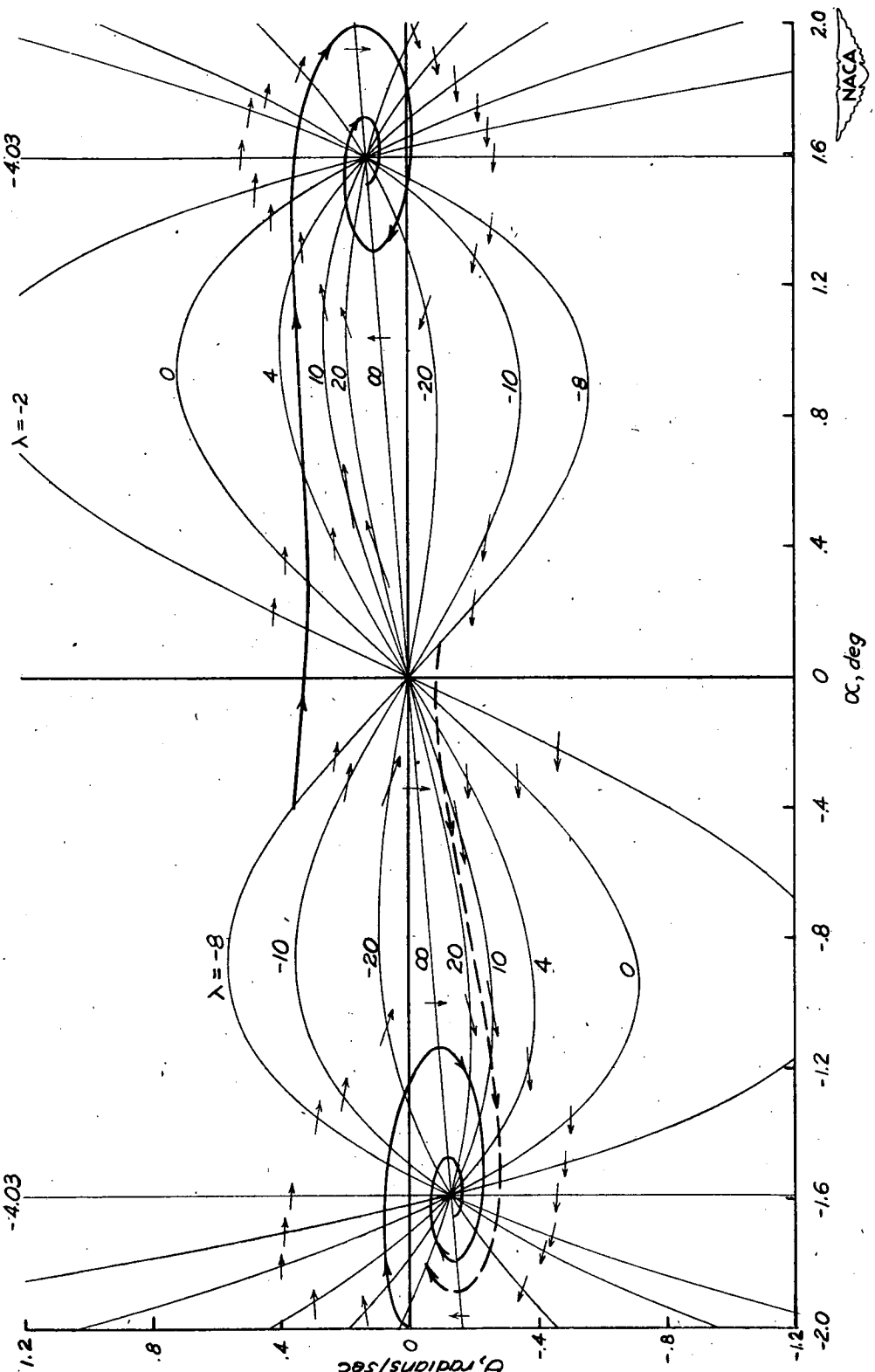

Figure 4.- The phase plane $(\alpha, \dot{\theta})$ for the example illustrating the methods of nonlinear mechanics. Three trajectories are shown; isoclines of constant λ are labeled.

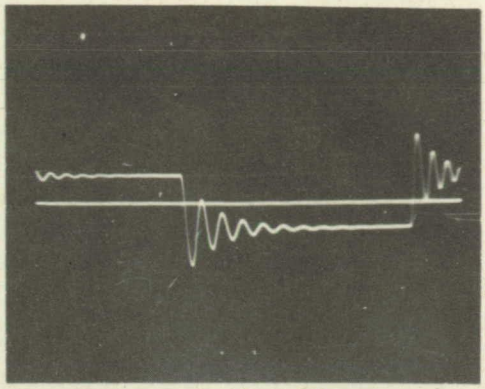

(a) Linear case, $\frac{dC_m}{d\alpha} = -5.14$.

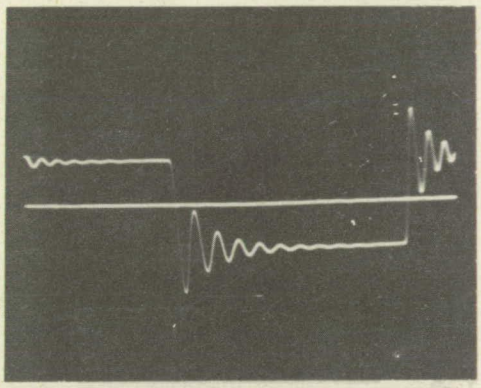

(b) α transient.

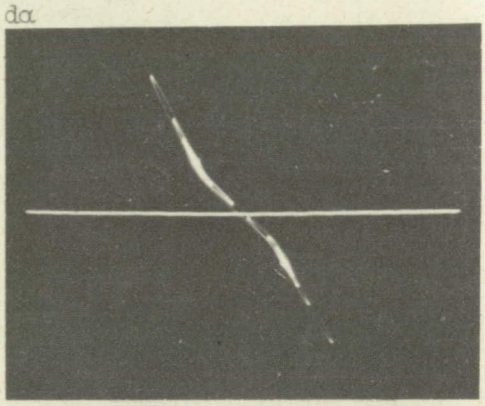

(c) Nonlinearity.

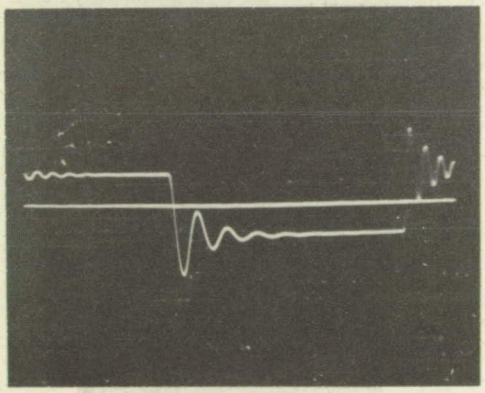

(d) α transient.

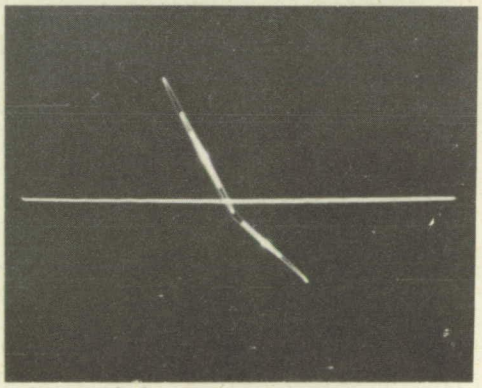

(e) Nonlinearity.

Figure 5.- Philbrick solutions for case I. Aircraft α transients and parts of nonlinearity involved; nonlinear $C_m(\alpha)$, $\frac{dC_m}{d\alpha} = -5.14$, $\alpha < -2^\circ$, $\alpha > 2^\circ$; $\frac{dC_m}{d\alpha} = -2.38$, $-2^\circ < \alpha < 2^\circ$; $\frac{dC_L}{d\alpha} = 3.49$, all α.

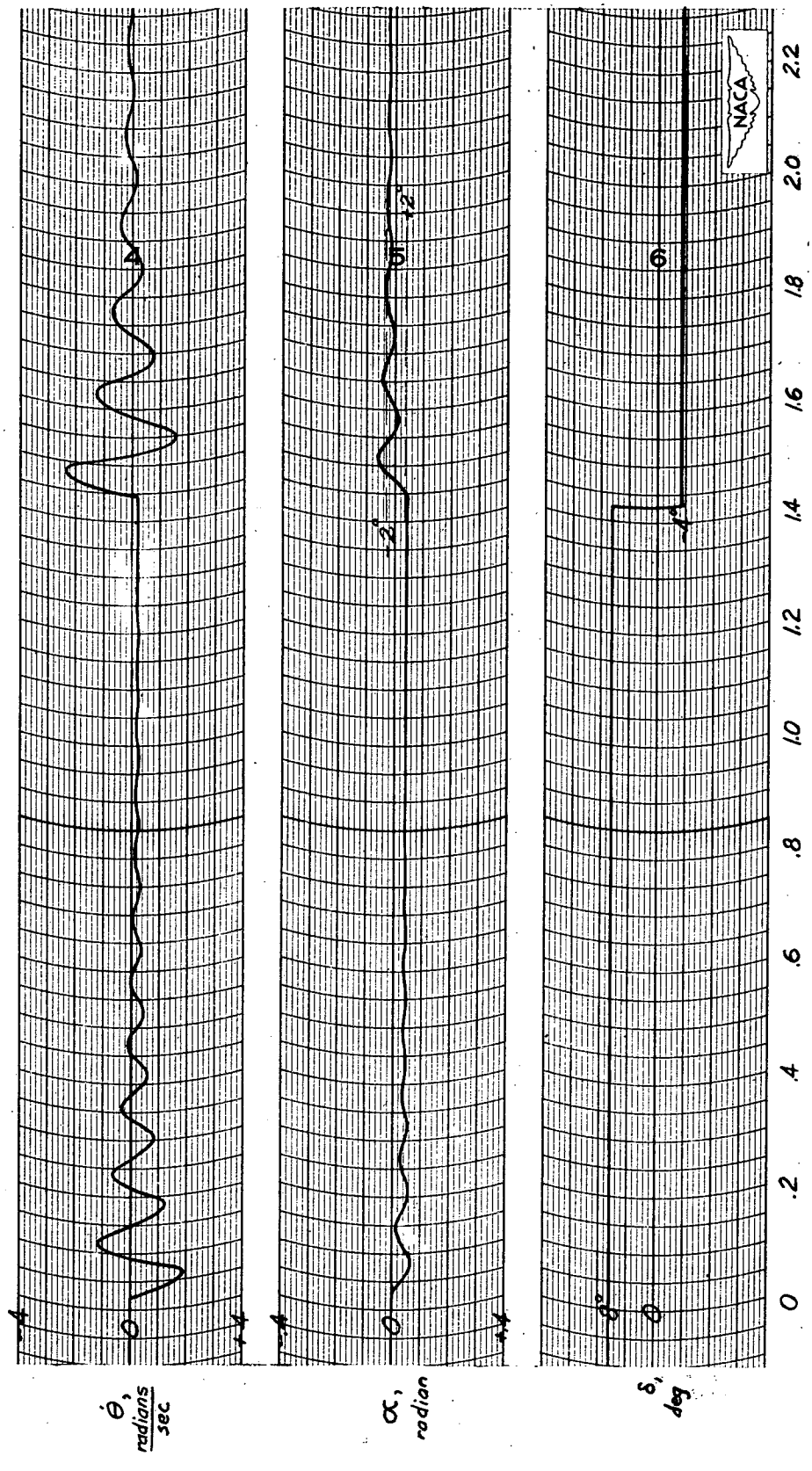

Figure 6.- REAC solutions for case I. Aircraft transients; nonlinear $C_m(\alpha)$ function with $\frac{dC_m}{d\alpha} = -6.0$, $\alpha < -2^\circ$, $\alpha > 2^\circ$; $\frac{dC_m}{d\alpha} = -3.0$, $-2^\circ < \alpha < 2^\circ$; $\frac{dC_L}{d\alpha} = 3.49$, all α.

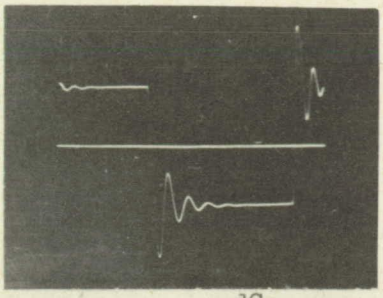

(a) Linear case, $\frac{dC_m}{d\alpha} = -0.838$.

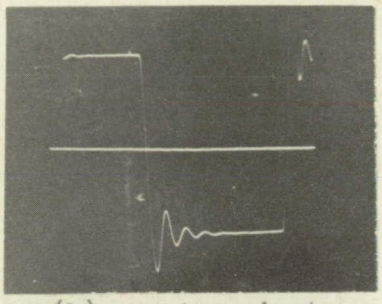

(b) α transient.

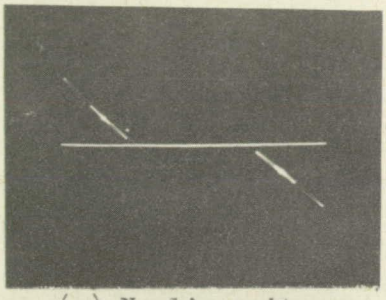

(c) Nonlinearity.

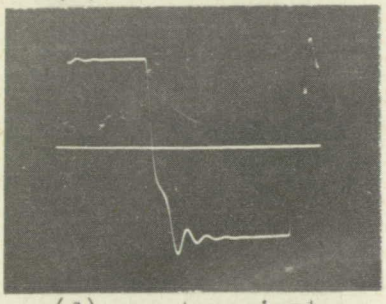

(d) α transient.

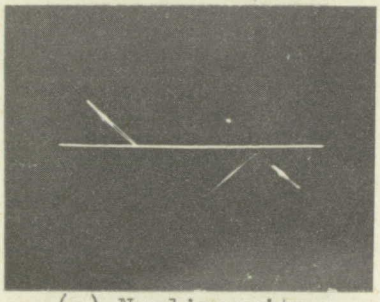

(e) Nonlinearity.

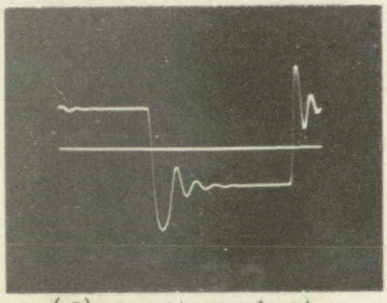

(f) α transient.

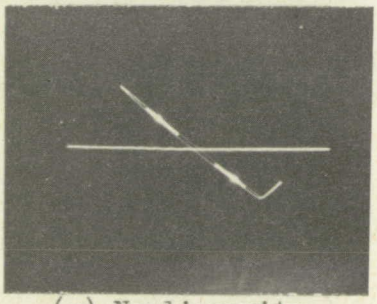

(g) Nonlinearity.

Figure 7.- Philbrick solutions for case II. Aircraft α transients and parts of nonlinearity involved; nonlinear $C_m(\alpha)$, $\frac{dC_m}{d\alpha} = -0.838$, $\alpha < -2^\circ$, $\alpha > 2^\circ$; $\frac{dC_m}{d\alpha} = 0.84$, $-2^\circ < \alpha < 2^\circ$; $\frac{dC_L}{d\alpha} = 3.49$, all α.

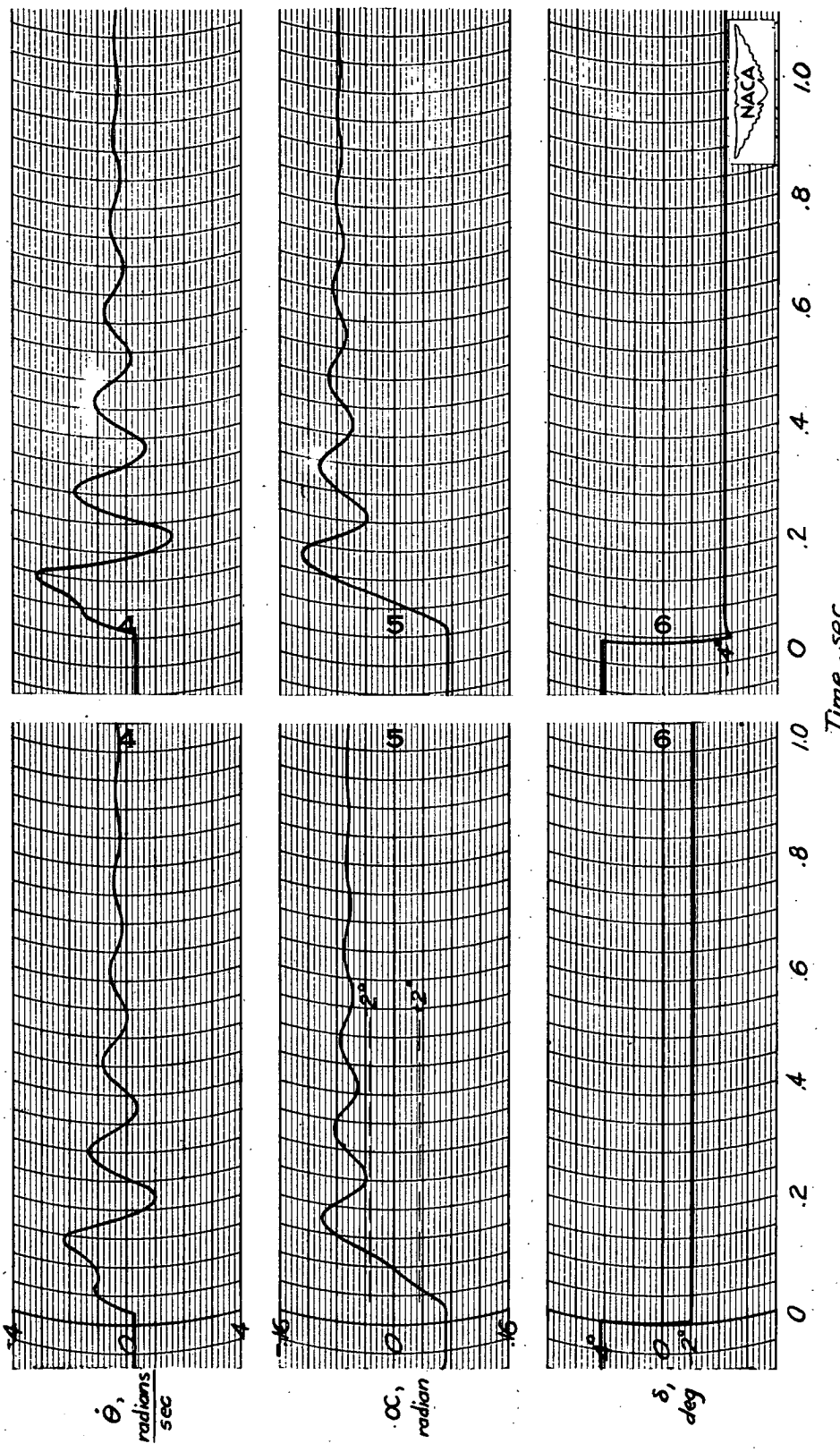

Figure 8.- REAC solutions for case II. Aircraft transients; nonlinear $C_m(\alpha)$ function with $\frac{dC_m}{d\alpha} = -3.0$, $\alpha < -2^\circ$, $\alpha > 2^\circ$; $\frac{dC_m}{d\alpha} = 1.5$, $-2^\circ < \alpha < 2^\circ$; $\frac{dC_L}{d\alpha} = 3.49$, all α.

PAGE MISSING FROM AVAILABLE VERSION

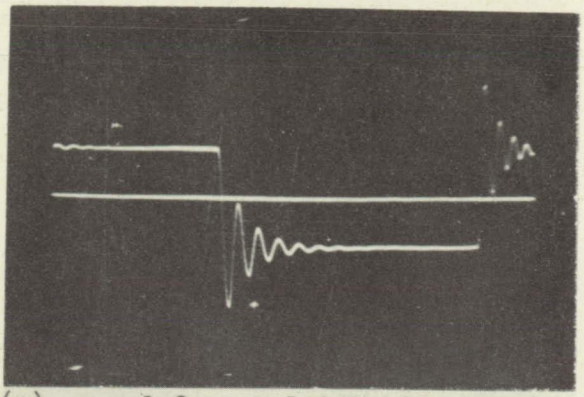

(a) n = 1.0, completely linear case.

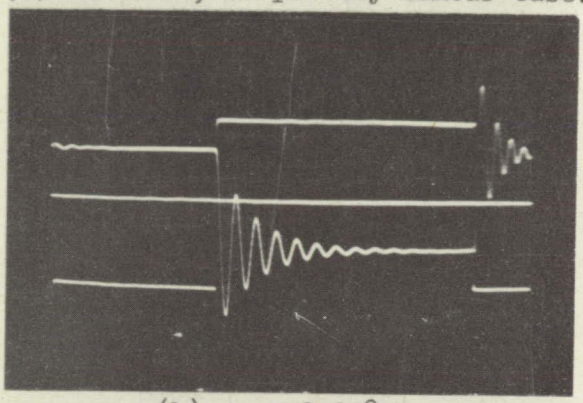

(b) n = 0.328.

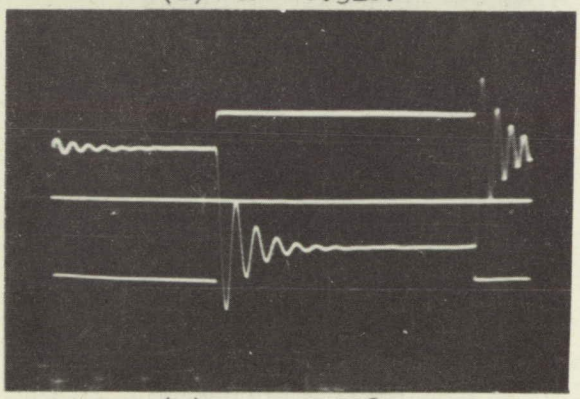

(c) n = 0.328.

Figure 9.- Philbrick solutions for case III. Aircraft α transients; nonlinear $C_L(\alpha)$; $\frac{dC_L}{d\alpha} = 3.49$, $\alpha < -2^\circ$, $\alpha > 2^\circ$; $\frac{dC_L}{d\alpha} = n(3.49)$, $-2^\circ < \alpha < 2^\circ$; $\frac{dC_m}{d\alpha} = -1.90$, all α.

PAGE MISSING FROM AVAILABLE VERSION

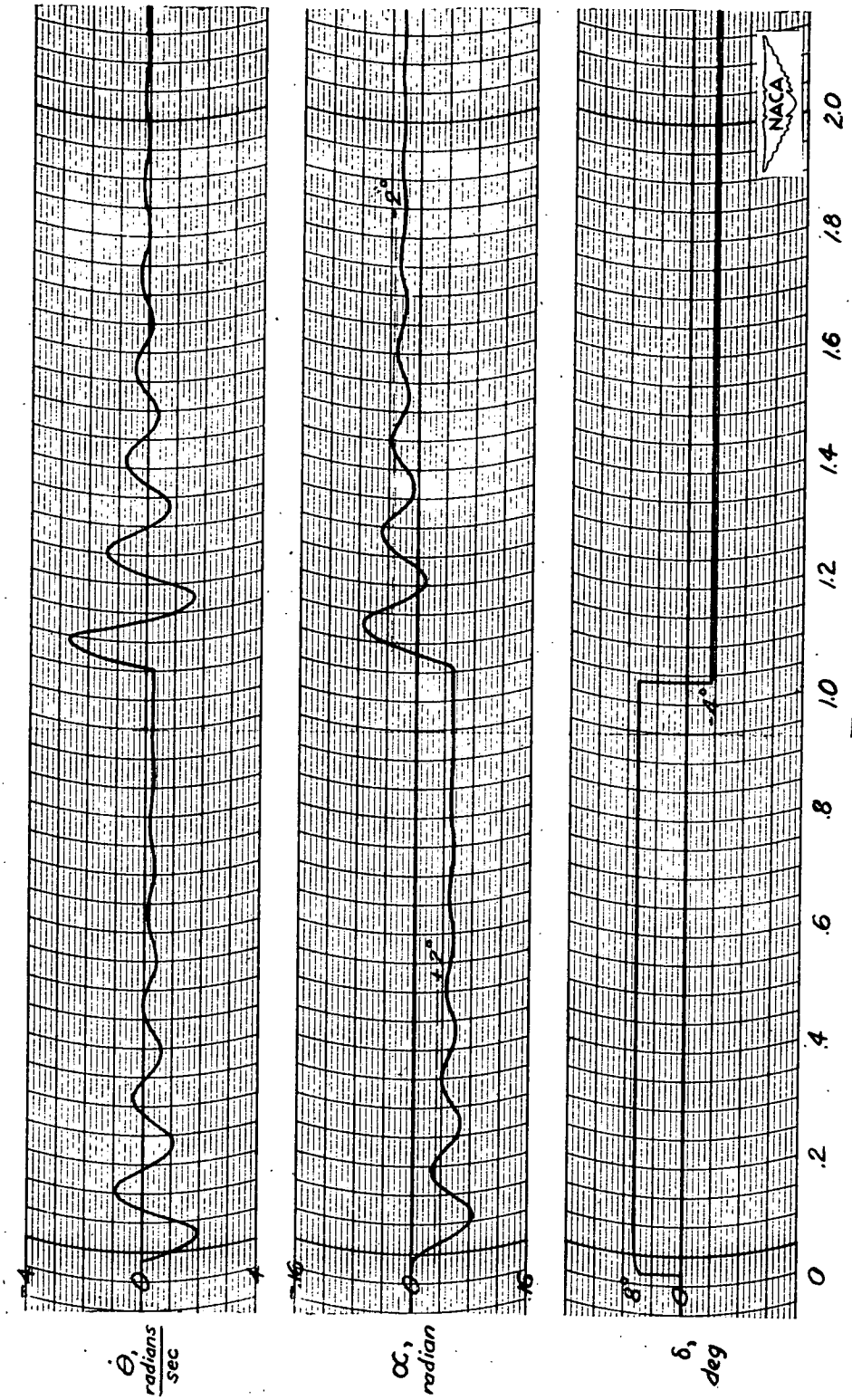

Figure 10.- REAC solutions for case III. Aircraft transients; nonlinear $C_L(\alpha)$ function with $\frac{dC_L}{d\alpha} = 4.19$, $\alpha < -2^\circ$, $\alpha > 2^\circ$; $\frac{dC_L}{d\alpha} = 3.49$, $-2^\circ < \alpha < 2^\circ$; $\frac{dC_m}{d\alpha} = -3.0$, all α.

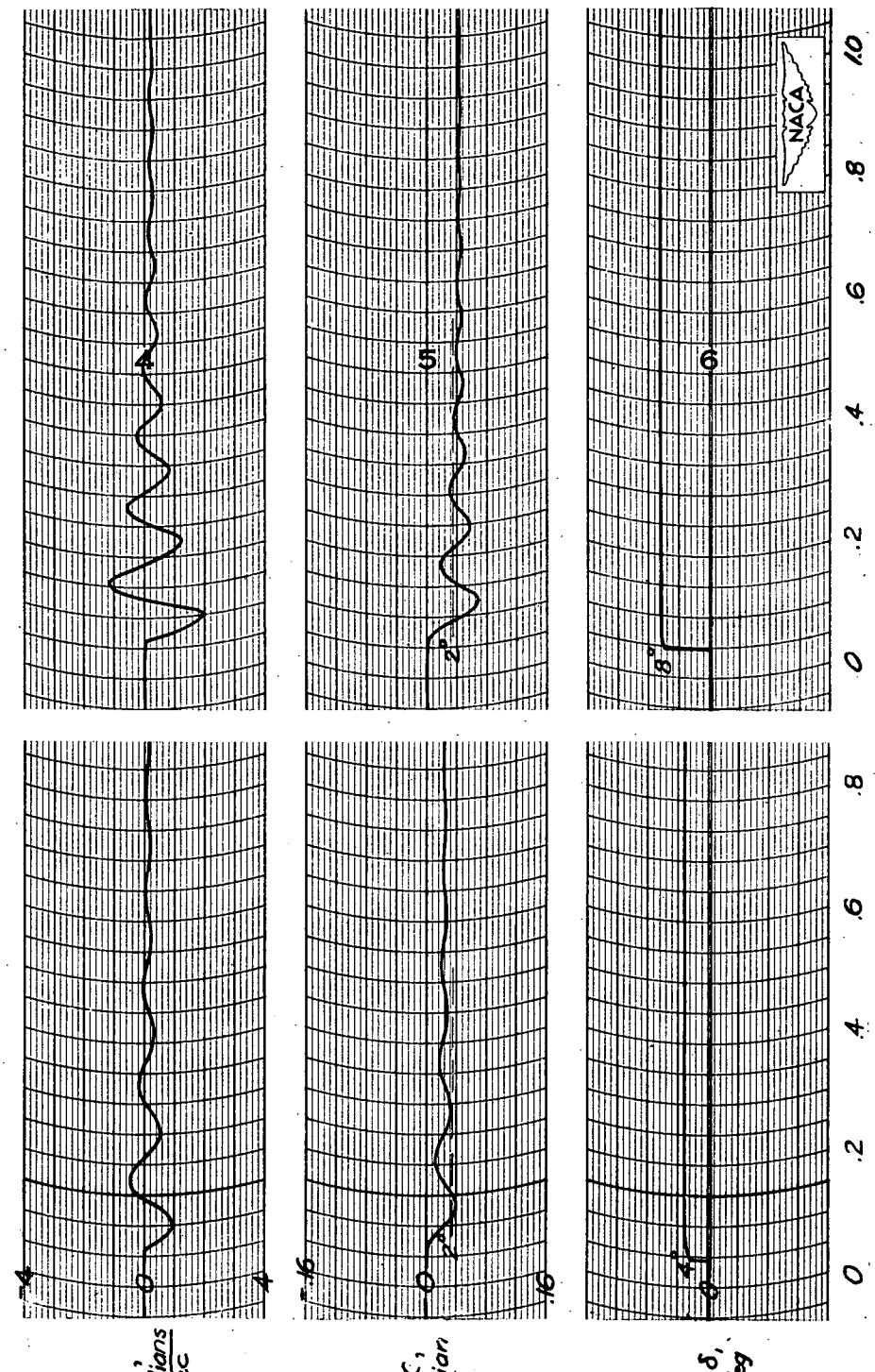

Figure 11.- REAC solutions for case IV. Aircraft transients; nonlinear $C_m(\alpha)$, $\frac{dC_m}{d\alpha} = -6.0$, $\alpha < -2^\circ$, $\alpha > 2^\circ$; $\frac{dC_m}{d\alpha} = -3.0$, $-2^\circ < \alpha < 2^\circ$; nonlinear $C_L(\alpha)$, $\frac{dC_L}{d\alpha} = 4.19$, $\alpha < -2^\circ$, $\alpha > 2^\circ$; $\frac{dC_L}{d\alpha} = 3.49$, $-2^\circ < \alpha < 2^\circ$.

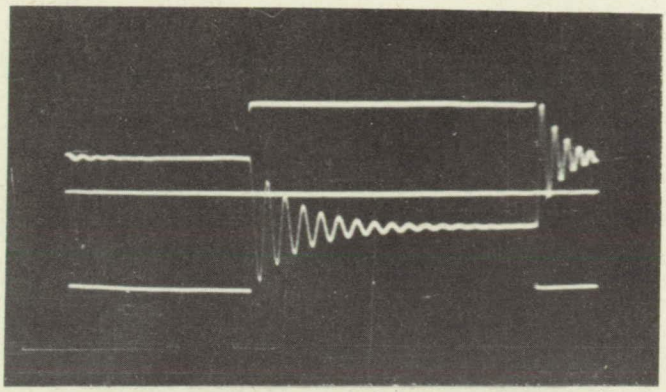

(a) Steady-state α in region where $\frac{dC_L}{d\alpha} = 1.14$.

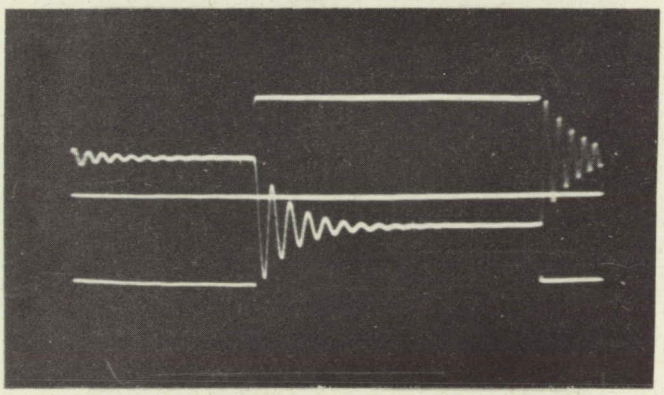

(b) Steady-state α in region where $\frac{dC_L}{d\alpha} = 3.49$.

Figure 12.- Philbrick solutions for proportional control system with angle-of-attack feedback. α transients, nonlinear $C_L(\alpha)$, $\frac{dC_L}{d\alpha} = 3.49$, $\alpha < -2^\circ$, $\alpha > 2^\circ$; $\frac{dC_L}{d\alpha} = 1.14$, $-2^\circ < \alpha < 2^\circ$; $\frac{dC_m}{d\alpha} = -1.90$, all α; autopilot constant $K_1 \approx 1.0$.

PAGE MISSING FROM AVAILABLE VERSION

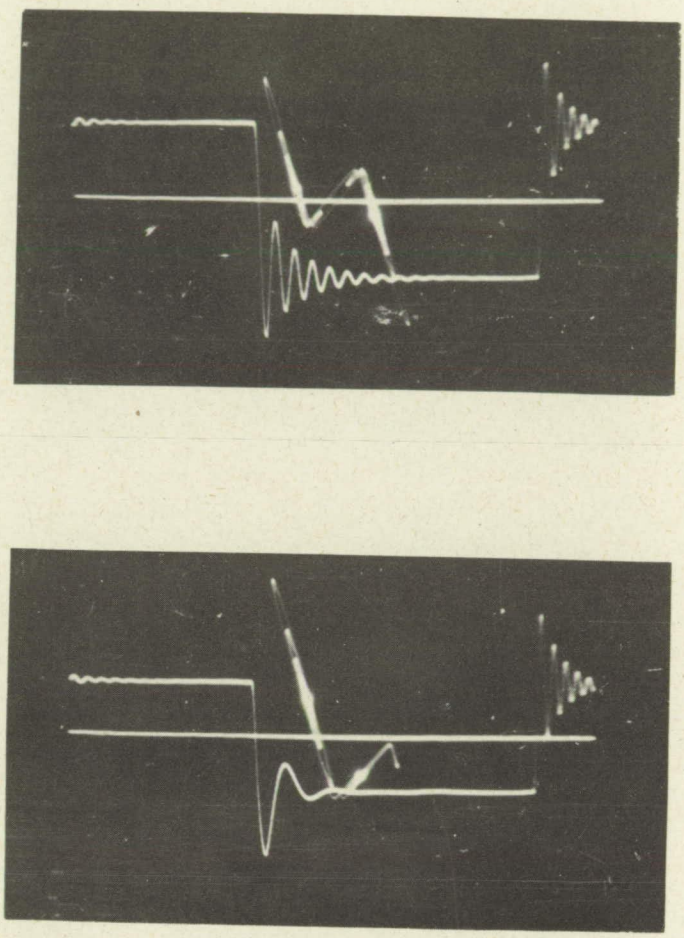

Figure 13.- Philbrick solutions for proportional control system with angle-of-attack feedback. α transients and parts of the nonlinearity; nonlinear $C_m(\alpha)$, $\frac{dC_m}{d\alpha} = -1.90$, $\alpha < -2^\circ$, $\alpha > 2^\circ$; $\frac{dC_m}{d\alpha} = 0.655$, $-2^\circ < \alpha < 2^\circ$; $\frac{dC_L}{d\alpha} = 3.49$, all α; autopilot constant $K_1 \approx 1.0$.

NACA

PAGE MISSING FROM AVAILABLE VERSION

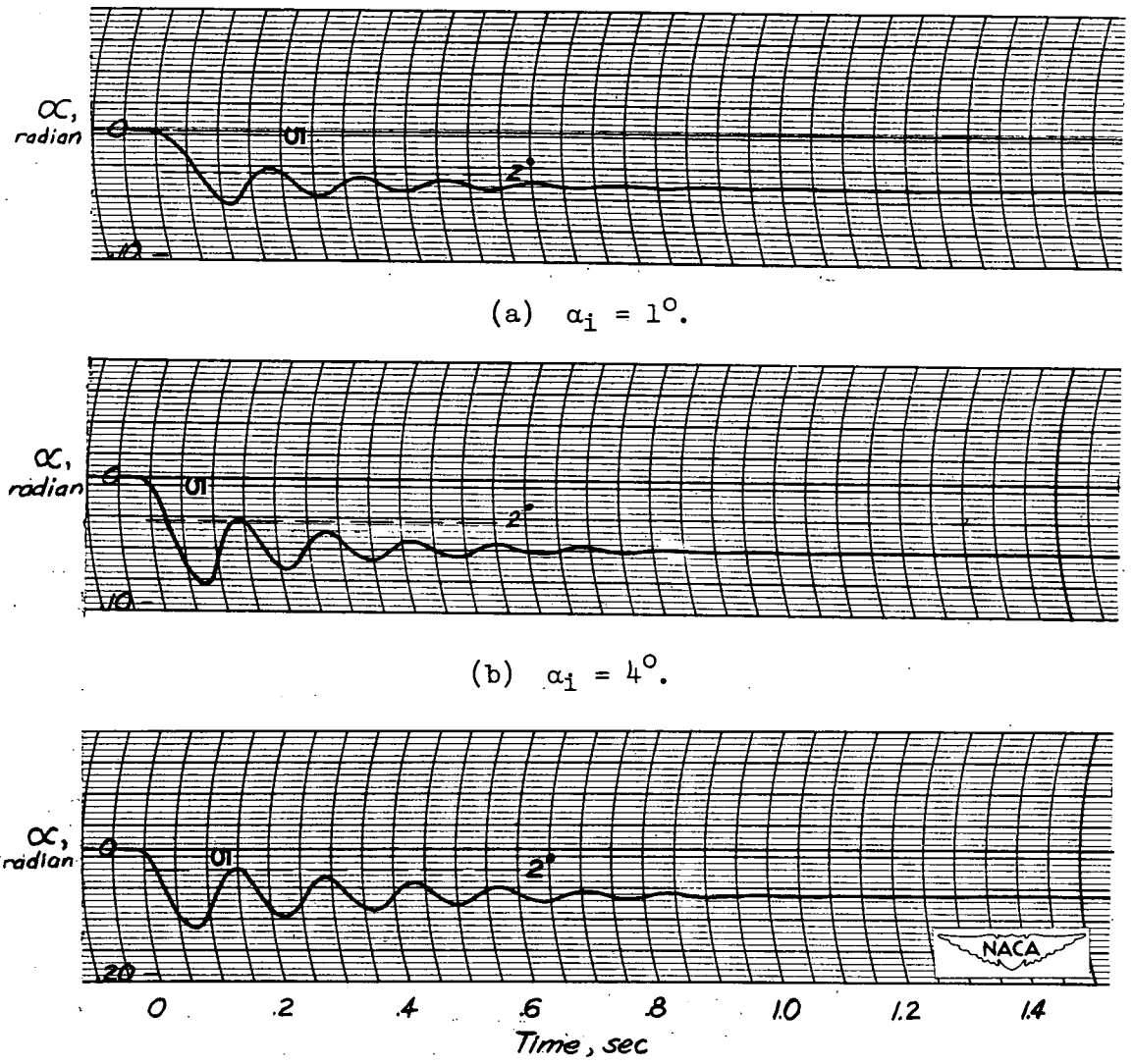

(a) $\alpha_i = 1^\circ$.

(b) $\alpha_i = 4^\circ$.

(c) $\alpha_i = 8^\circ$.

Figure 14.- REAC solutions for proportional control system with angle-of-attack feedback. Nonlinear $C_m(\alpha)$, $\frac{dC_m}{d\alpha} = 1.5$, $-2^\circ < \alpha < 2^\circ$; $\frac{dC_m}{d\alpha} = -3.0$, $\alpha < -2^\circ$, $\alpha > 2^\circ$; $\frac{dC_L}{d\alpha} = 3.49$, all α; autopilot constant $K_1 = 1.0$.

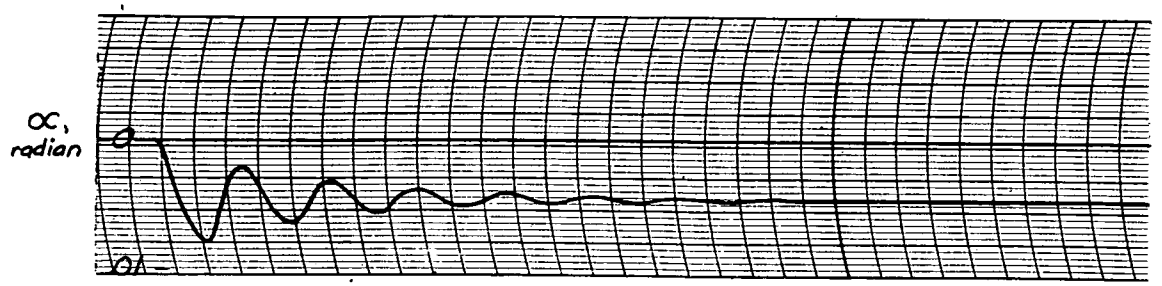

(a) $\alpha_i = 1^\circ$.

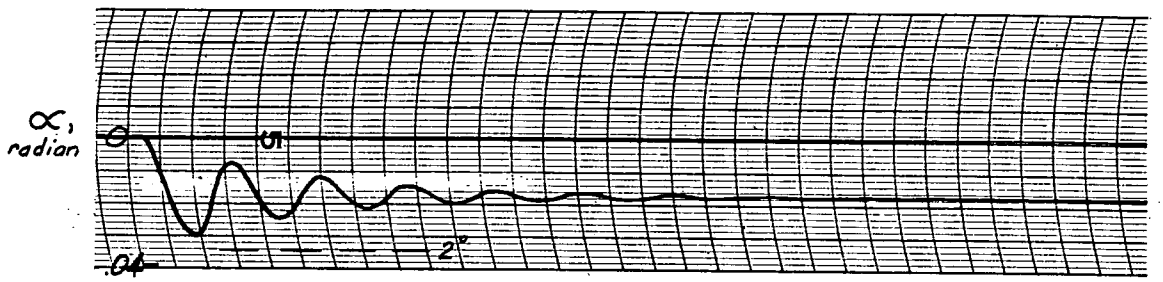

(b) $\alpha_i = 4^\circ$.

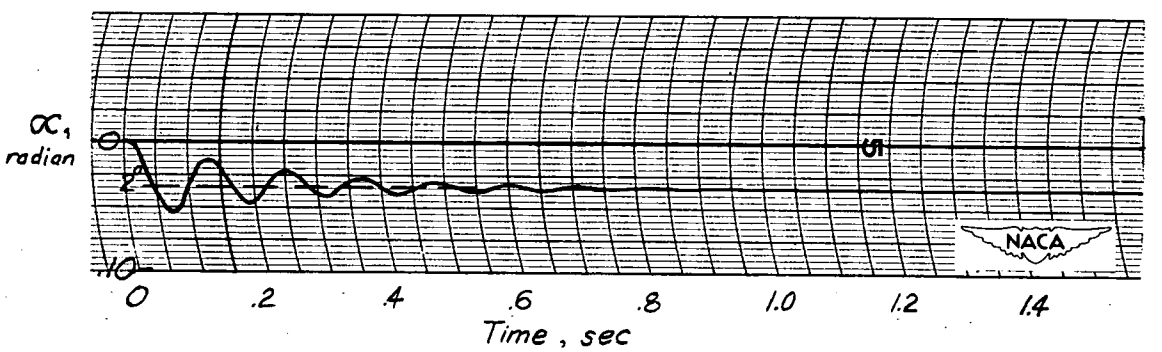

(c) $\alpha_i = 8^\circ$.

Figure 15.- REAC solutions for proportional control system with angle-of-attack feedback. Nonlinear $C_m(\alpha)$, $\frac{dC_m}{d\alpha} = -3.0$, $-2^\circ < \alpha < 2^\circ$; $\frac{dC_m}{d\alpha} = -6.0$, $\alpha < -2^\circ$, $\alpha > 2^\circ$; $\frac{dC_L}{d\alpha} = 3.49$, all α; autopilot constant $K_1 = 1.0$.

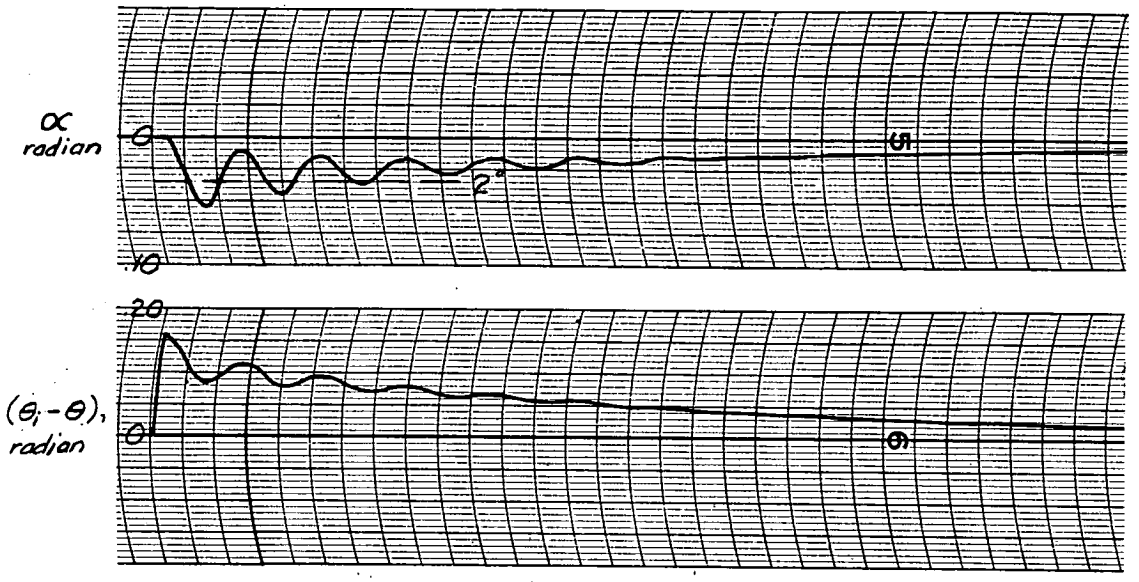

(b) $\theta_i = 9^\circ$.

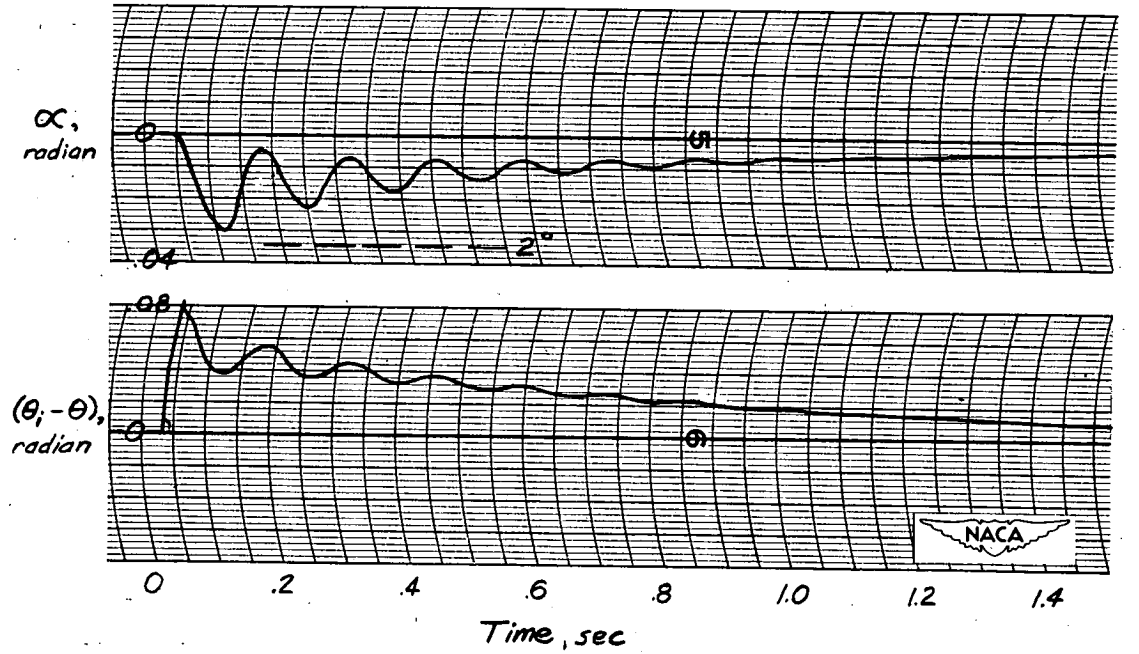

(a) $\theta_i = 4.6^\circ$.

Figure 16.- REAC solutions for proportional control for attitude stabilization. Nonlinear $C_m(\alpha)$, $\frac{dC_m}{d\alpha} = -3.0$, $-2^\circ < \alpha < 2^\circ$; $\frac{dC_m}{d\alpha} = -6.0$, $\alpha < -2^\circ$, $\alpha > 2^\circ$; $\frac{dC_L}{d\alpha} = 3.49$; autopilot constant $K_2 = 1.0$.

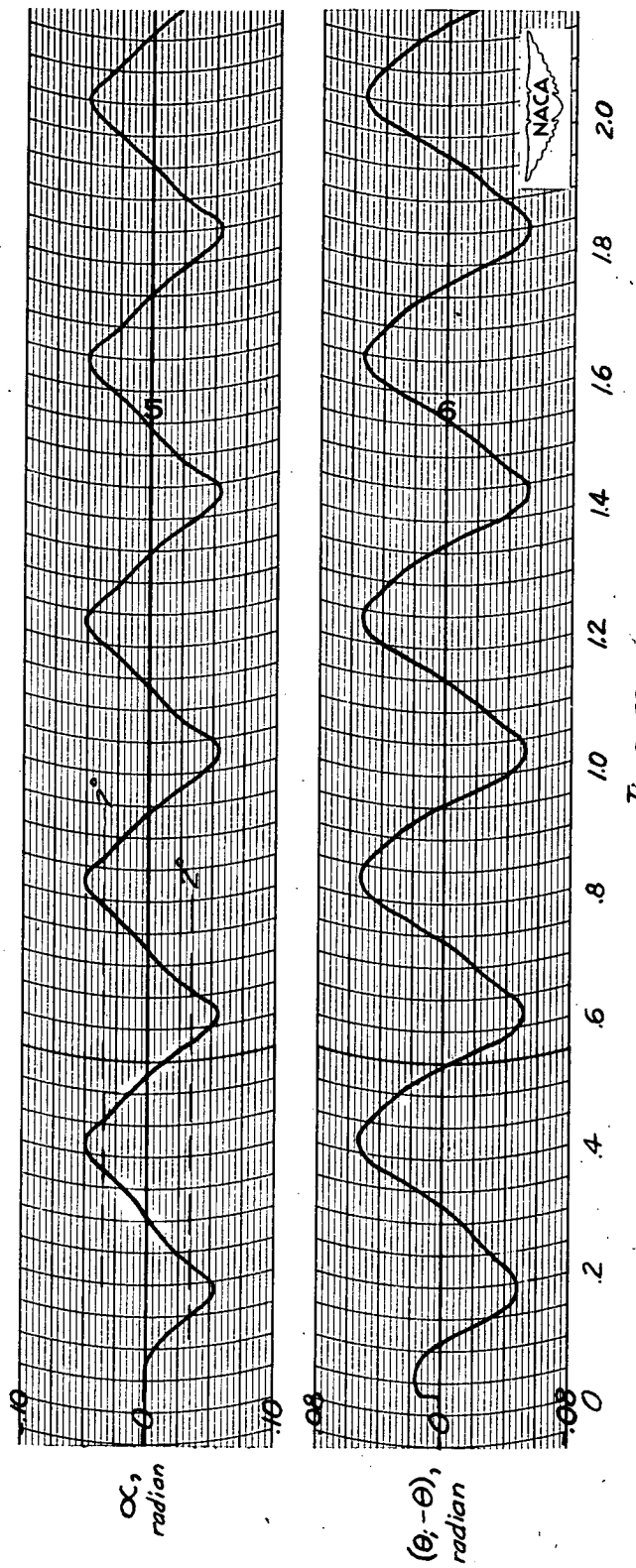

(a) $\theta_1 = 0.7^\circ$.

Figure 17.- REAC solutions for proportional control for attitude stabilization. Nonlinear $C_m(\alpha)$, $\frac{dC_m}{d\alpha} = 1.5$, $-2^\circ < \alpha < 2^\circ$; $\frac{dC_m}{d\alpha} = -3.0$, $\alpha < -2^\circ$, $\alpha > 2^\circ$; $\frac{dC_L}{d\alpha} = 3.49$; autopilot constant $K_2 = 1.0$.

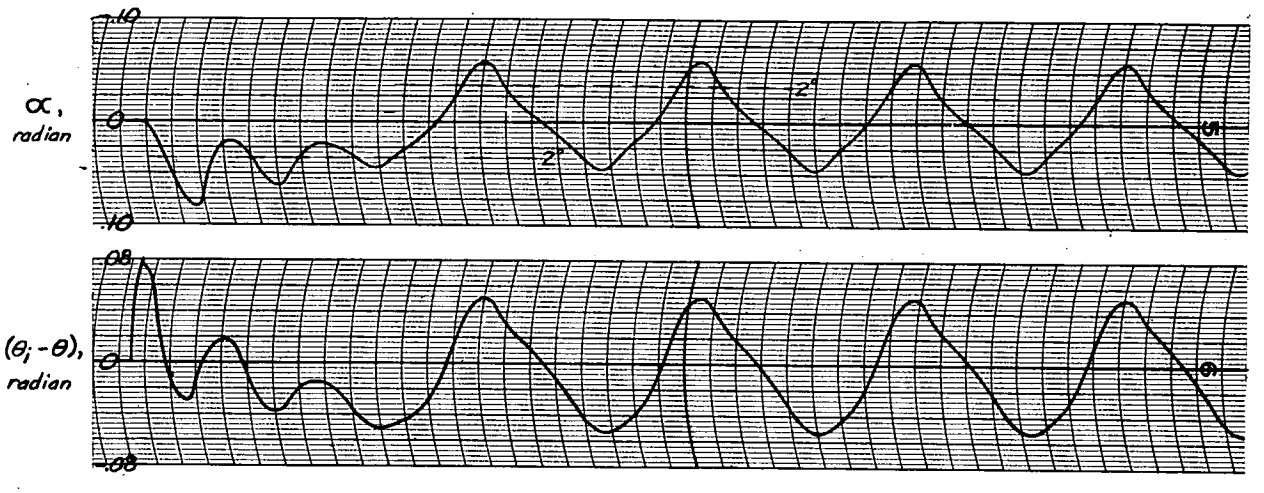

(b) $\theta_i = 4.6°$.

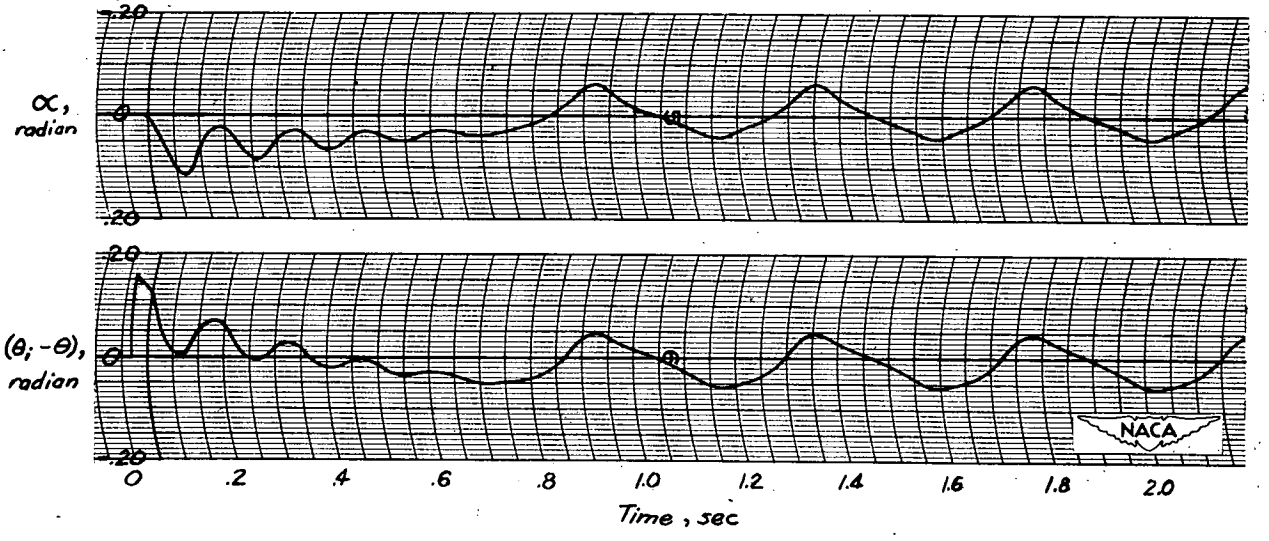

(c) $\theta_i = 8.7°$.

Figure 17.- Concluded.